Journal of Computational Physics 303 (2015) 146–172

Contents lists available at ScienceDirect

Journal of Computational Physics

www.elsevier.com/locate/jcp

# Implicit, semi-analytical solution of the generalized Riemann problem for stiff hyperbolic balance laws

Eleuterio F. Toro [a], Gino I. Montecinos [b,*]

[a] Laboratory of Applied Mathematics, DICAM, University of Trento, Trento, Italy
[b] Center for Mathematical Modeling (CMM), Universidad de Chile, Santiago, Chile

ARTICLE INFO

*Article history:*
Received 24 April 2015
Received in revised form 10 September 2015
Accepted 22 September 2015
Available online 28 September 2015

*Keywords:*
Hyperbolic balance laws
Stiff source terms
Generalized Riemann problem
Cauchy–Kowalewskaya procedure
High-order ADER schemes

ABSTRACT

We present a semi-analytical, implicit solution to the generalized Riemann problem (GRP) for non-linear systems of hyperbolic balance laws with stiff source terms. The solution method is based on an implicit, time Taylor series expansion and the Cauchy–Kowalewskaya procedure, along with the solution of a sequence of classical Riemann problems. Our new GRP solver is then used to construct *locally implicit ADER methods* of arbitrary accuracy in space and time for solving the general initial–boundary value problem for non-linear systems of hyperbolic balance laws with stiff source terms. Analysis of the method for model problems is carried out and empirical convergence rate studies for suitable tests problems are performed, confirming the theoretically expected high order of accuracy.



## 1. Introduction

This paper is motivated by the fully discrete one-step ADER approach to construct numerical schemes of arbitrarily high order of accuracy in space and time for solving hyperbolic equations. ADER (Arbitrary Accuracy DERivative Riemann problem method) was first put forward by Toro et al. [41], in the finite volume framework, for solving linear hyperbolic equations in one and multiple space dimensions on Cartesian meshes; see also Schwartzkopff, Munz and Toro [35]. The extension of finite volume ADER schemes (ADER-FV) to non-linear equations, due to Titarev and Toro [38], is based on a semi-analytical, explicit solution of the Generalized Riemann problem put forward by Toro and Titarev [43]. Since then, ADER has also been extended to the discontinuous Galerkin finite element framework by Dumbser [17], giving rise to ADER-DG schemes. For an elementary introduction to ADER schemes and the generalized Riemann problem, the reader is referred to Chapters 19 and 20 of the textbook by Toro [40]. Further generalizations were put forward by Dumbser et al. [17], setting ADER-FV and ADER-DG in a generalized framework. Subsequently, Dumbser et al. [11] proposed a unified framework for the ADER approach as applied to general non-linear hyperbolic systems with stiff and non-stiff source terms. The resulting family of ADER numerical schemes has been called $P_N P_M$ methods, where $N$ indicates the degree of test function polynomials and $M$ the degree of polynomials used for flux and source term evaluations. For $N = 0$ one reproduces the original ADER-FV schemes and for $N = M$ one reproduces the ADER-DG method. $P_N P_M$ schemes were later extended to general non-linear viscous PDEs in [12,10]. The ADER approach has undergone numerous extensions and applications, further examples include [7,24–26,37–39,43,44,17,9,18,15,16,2,1,32–34,29,19,20,14,42,4,6,5].

* Corresponding author.
*E-mail address:* gmontecinos@dim.uchile.cl (G.I. Montecinos).

http://dx.doi.org/10.1016/j.jcp.2015.09.039
0021-9991/

ADER methods are one-step, fully discrete schemes, containing two main ingredients, namely (i) a high-order, non-linear spatial reconstruction procedure and (ii) solution of a generalized Riemann problem at each cell interface to compute the *numerical flux* to high order of accuracy. In this manner, for homogeneous hyperbolic systems, the finite volume ADER method is completely determined. We note that step (i) is not required for ADER DG schemes. For hyperbolic balance laws one needs an additional step to compute the *numerical source* to high order of accuracy. This is achieved by solving local Cauchy problems to high order inside space–time control volumes. Note that for finite volume ADER schemes the spatial reconstruction in step (i) must be non-linear, in order to circumvent Godunov's theorem [21,40] and control spurious oscillations. The basic building block of ADER schemes is step (ii), namely the solution of the generalized Riemann problem to compute the *numerical flux*. Several ways of solving the GRP have been recently reported; for a review see Montecinos et al. [30]. The first solver, due to Toro and Titarev [43], was inspired by the second-order GRP method of Ben-Artzi and Falcoviz [3]; the method finds a time-dependent Godunov state right at the cell interface via an *explicit* time Taylor series expansion as proposed by Le Floch and Raviart [27]. To complete the solution Toro and Titarev employed the Cauchy–Kowalewskaya procedure to convert time derivatives in the series to functionals of space derivatives. Then, to find these space derivatives, they solved classical Riemann problems for space derivatives, completely determining the Taylor expansion for the time-dependent Godunov state. In [22] it has been proved for the scalar case that the procedure of Toro and Titarev, reproduces exactly the Taylor series expansion of Le Floch and Raviart [27]. The numerical flux is finally computed as an integral average of this Godunov state. Later, Castro and Toro [8] reinterpreted the high-order Godunov type method due to Harten et al. [23], as an ADER-type scheme with a particular way of solving the generalized Riemann solver, which they called the HEOC solver for the GRP. Castro and Toro also proposed another way of solving the GRP, analogous to that of Toro and Titarev, and showed that for linear systems all three GRP solvers are algebraically identical. ADER methods with all the three solvers for the GRP produce schemes of arbitrary order of accuracy, in space and time, for hyperbolic balance laws with *non-stiff source terms*. In the presence of stiff source terms the methods fail to be of practical use. This limitation of ADER schemes was overcome with the advent of an *implicit* solver for the GRP for hyperbolic balance laws with *stiff source terms*, proposed by Dumbser, Enaux and Toro [13]. This GRP solver, called the DET solver, may be seen as a numerical interpretation/extension of the HEOC solver. Instead of Taylor expanding the limiting values, from left and right of the interface, of the piecewise smooth initial data, one solves the Cauchy problem numerically with an implicit (local) space–time DG method and then interacts the evolved data as in the HEOC solver. The resulting explicit ADER schemes are able to reconcile stiffness and high accuracy via this (locally) implicit numerical solver for the GRP.

In this paper we present a new, implicit semi-analytical solution to the generalized Riemann problem for systems of balance laws with stiff source terms. When this solution is implemented in the ADER framework, one obtains explicit one-step methods of arbitrary order of accuracy with a (locally) implicit solver for the GRP. The schemes are able to solve the general initial boundary value problem with stiff source terms. The new solver is the implicit version of the Toro–Titarev solver [43] and is based on an implicit Taylor series expansion leading to a, local, non-linear algebraic system to find the time-dependent Godunov state. The new implicit solver is an extension to partial differential equations with stiff source terms of the implicit method proposed by Scott [36] for solving stiff ordinary differential equations. The associated implicit Taylor series expansion is a generalization of that proposed by Le Floch and Raviart [27]. The present implicit GRP solver can be implemented in the ADER framework by directly seeking a time-dependent Godunov state right at the interface, as in [43]. This requires one Taylor series expansion right at the interface. A second possibility is to follow the HEOC solver [23,8], whereby two Taylor expansions are required, one on each side of the interface. In the present paper we implement both approaches and systematically evaluate their performance. The methods are analysed for model problems and a convergence rates study is carried out to ensure that the theoretically expected orders of accuracy are actually attained.

The rest of this paper is organised as follows: in Section 2 we present ADER type schemes and briefly review conventional solvers for the associated generalized Riemann problem (GRP). In Section 3 we introduce the new solver for the GRP. In Section 4 we present some theoretical and numerical results regarding the new GRP solver. In Section 5 we construct ADER schemes based on the new GRP solver and a systematic convergence rates assessment is carried out for several test problems for non-linear problems. Conclusions are found in Section 6.

## 2. Brief review of ADER and GRP solvers

A succinct review of the ADER approach, in the frame of the finite volume method, is presented here.

### 2.1. The finite volume framework and ADER schemes

Let us consider a general system of hyperbolic balance laws

$$\partial_t \mathbf{Q}(x,t) + \partial_x \mathbf{F}(\mathbf{Q}(x,t)) = \mathbf{S}(\mathbf{Q}(x,t)) \,, \tag{1}$$

where $\mathbf{Q} \in \mathbf{R}^m$ is the vector of conserved variables, the unknowns of the problem, $\mathbf{F}(\mathbf{Q})$ is the physical flux and $\mathbf{S}(\mathbf{Q})$ is the source term. Direct integration of (1) in the space–time control volume $V_i^n = \left[x_{i-\frac{1}{2}}, x_{i+\frac{1}{2}}\right] \times \left[t^n, t^{n+1}\right]$ yields

$$\mathbf{Q}_i^{n+1} = \mathbf{Q}_i^n - \frac{\Delta t}{\Delta x}\left[\mathbf{F}_{i+\frac{1}{2}} - \mathbf{F}_{i-\frac{1}{2}}\right] + \Delta t \mathbf{S}_i \,, \tag{2}$$

with

$$\left.\begin{aligned} \mathbf{Q}_i^n &= \frac{1}{\Delta x}\int_{x_{i-\frac{1}{2}}}^{x_{i+\frac{1}{2}}} \mathbf{Q}(x,t^n)dx\,, \\ \mathbf{F}_{i+\frac{1}{2}} &= \frac{1}{\Delta t}\int_{t^n}^{t^{n+1}} \mathbf{F}\left(\mathbf{Q}(x_{i+\frac{1}{2}},t)\right)dt\,, \\ \mathbf{S}_i &= \frac{1}{\Delta t\Delta x}\int_{t^n}^{t^{n+1}}\int_{x_{i-\frac{1}{2}}}^{x_{i+\frac{1}{2}}} \mathbf{S}\left(\mathbf{Q}(x,t)\right)dxdt\,. \end{aligned}\right\} \tag{3}$$

Formula (2) is exact if integrals (3) are exact. Finite volume methods depart from an approximate interpretation of (2), with approximations for (3). We shall still use formula (2) but understood it as a finite volume formula for numerical purposes. ADER type methods aim at evaluating the integrals (3) to high order of accuracy, resulting in explicit, one-step high order numerical methods (2) to solve (1). Note that only the second and third integrals in (3) are required throughout the space time domain, while the first integral is computed only at the initial time. ADER schemes are a generalization of Godunov's method and are based on two building blocks: (i) a non-linear reconstruction procedure and (ii) solution of a local generalized Riemann problem at each cell interface for flux evaluation. In the presence of source terms one requires an additional procedure to evaluate the volume integral in (3), for which additional Cauchy problem solutions are required within the space–time control volume. In the next section we introduce these Cauchy problems.

### 2.2. The generalized Riemann problem

The Generalized Riemann Problem (GRP) for (1) is the Cauchy problem

$$\left.\begin{aligned} &\partial_t\mathbf{Q}(x,t)+\partial_x\mathbf{F}(\mathbf{Q}(x,t))=\mathbf{S}(\mathbf{Q}(x,t))\,, \\ &\mathbf{Q}(x,0)=\begin{cases}\mathbf{P}_L(x), & x<0\,,\\ \mathbf{P}_R(x), & x>0\,,\end{cases} \end{aligned}\right\} \tag{4}$$

with $\mathbf{P}_L(x)$ and $\mathbf{P}_R(x)$ smooth functions, which for the ADER-FV come from the reconstruction procedure. Note that one only requires the solution along the interface position $x=0$, as a function of time. We denote this solution by $\mathbf{Q}_{LR}(\tau)$, which is used for flux evaluation, namely

$$\mathbf{F}_{i+\frac{1}{2}} = \frac{1}{\Delta t}\int_0^{\Delta t}\mathbf{F}(\mathbf{Q}_{LR}(\tau))d\tau\,. \tag{5}$$

The source term is computed approximately through a quadrature rule defined in $[x_{i-\frac{1}{2}}, x_{i+\frac{1}{2}}]$ given as

$$\mathbf{S}_i = \sum_{j=1}^{K}\frac{w_j}{\Delta t}\int_0^{\Delta t}\mathbf{S}(\mathbf{Q}_\mathbf{j}(\tau)dt)\,, \tag{6}$$

where $w_j$ are the weights associated to the spatial quadrature points $x=\xi_j$ and $\mathbf{Q}_j(\tau)$ is the time-dependent solution at $x=\xi_j$ and is the solution of the initial-value problem

$$\left.\begin{aligned} &\partial_t\mathbf{Q}(x,t)+\partial_x\mathbf{F}(\mathbf{Q}(x,t))=\mathbf{S}(\mathbf{Q}(x,t))\,, \\ &\mathbf{Q}(x,0)=\mathbf{P}_L(x)\,. \end{aligned}\right\} \tag{7}$$

We remark that the strategy to solve the Generalized Riemann Problem (4) can also be used to solve (7) and compute $\mathbf{Q}_j(\tau)$ in (6).

Next, we briefly review existing solvers for (4), based on Taylor series expansions and the Cauchy–Kowalewskaya procedure, whereby time derivatives are expressed as functionals of space derivatives, namely

$$\partial_t^{(k)}\mathbf{Q}(x,t)=\mathbf{G}^{(k)}(\mathbf{Q}(x,t),\ldots,\partial_x^{(k)}\mathbf{Q}(x,t))\,. \tag{8}$$

$\mathbf{G}^{(k)}$ will be called the Cauchy–Kowalewskaya functional. In what follows we shall briefly review two existing GRP solvers that are relevant to the present paper.

### 2.3. The Toro–Titarev (TT) solver

Following [27] and [43], the solution $\mathbf{Q}_{LR}(\tau)$ is expressed in terms of a Taylor series expansion in time

$$\mathbf{Q}_{LR}(\tau) = \mathbf{Q}(0,0_+) + \sum_{k=1}^{M} \frac{\tau^k}{k!} \partial_t^{(k)} \mathbf{Q}(0,0_+) \,. \tag{9}$$

From (8), time derivatives $\partial_t^{(k)}\mathbf{Q}$ are replaced by their respective Cauchy–Kowalewskaya functional $\mathbf{G}^{(k)}$

$$\partial_t^{(k)} \mathbf{Q}(0,0_+) = \mathbf{G}^{(k)}(\mathbf{Q}(0,0_+), \ldots, \partial_x^{(k)} \mathbf{Q}(0,0_+)) \,, \tag{10}$$

where $\partial_t^{(k)}\mathbf{Q}(0,0_+) = \lim_{t\to 0_+} \partial_t^{(k)}\mathbf{Q}(0,t)$, with $k = 0, 1, \ldots, M$ and $\partial_t^{(0)}\mathbf{Q} = \mathbf{Q}$.

The leading term $\mathbf{Q}(0,0_+)$ is found as the self-similar solution of the classical Riemann problem

$$\left.\begin{aligned} &\partial_t \mathbf{Q} + \partial_x \mathbf{F}(\mathbf{Q}) = \mathbf{0} \,, \\ &\mathbf{Q}(x,0) = \begin{cases} \mathbf{P}_L(0_-) = \lim\limits_{x\to 0_-} \mathbf{P}_L(x) & x < 0 \,, \\ \mathbf{P}_R(0_+) = \lim\limits_{x\to 0_+} \mathbf{P}_R(x) & x > 0 \,. \end{cases} \end{aligned}\right\} \tag{11}$$

High-order spatial derivatives are found as self-similar solutions of the following classical, derivative Riemann problems

$$\left.\begin{aligned} &\partial_t \left(\partial_x^{(k)}\mathbf{Q}\right) + \mathbf{A}(\mathbf{Q}(0,0_+))\partial_x \left(\partial_x^{(k)}\mathbf{Q}\right) = \mathbf{0} \,, \\ &\partial_x^{(k)}\mathbf{Q}(x,0) = \begin{cases} \mathbf{P}_L^{(k)}(0_-) = \lim\limits_{x\to 0_-} \dfrac{d^k}{dx^k}\mathbf{P}_L(x) & x < 0 \,, \\ \mathbf{P}_R^{(k)}(0_+) = \lim\limits_{x\to 0_+} \dfrac{d^k}{dx^k}\mathbf{P}_R(x) & x > 0 \,, \end{cases} \end{aligned}\right\} \tag{12}$$

where $\mathbf{A}(\mathbf{Q})$ is the Jacobian matrix evaluated at the leading term in (9). Details on the evolution equations in (12) for spatial derivatives are found in [43]. Note that this solver requires the solution of one non-linear classical Riemann problem for the leading term and a sequence of classical linear Riemann problems for the spatial derivatives.

### 2.4. The Harten–Engquist–Osher–Chakravarthy (HEOC) solver

Here we review the Castro and Toro [8] reinterpretation of the Harten et al. method [23] in terms of a local GRP. The GRP solution $\mathbf{Q}_{LR}(\tau)$ at each time $\tau$ is found as the self-similar solution of the associated classical Riemann problem

$$\left.\begin{aligned} &\partial_t \mathbf{Q} + \partial_x \mathbf{F}(\mathbf{Q}) = \mathbf{0} \,, \\ &\mathbf{Q}(x,0) = \begin{cases} \hat{\mathbf{Q}}_L(\tau) & x < 0 \,, \\ \hat{\mathbf{Q}}_R(\tau) & x > 0 \,, \end{cases} \end{aligned}\right\} \tag{13}$$

evaluated at the interface $x/t = 0$. Here $\hat{\mathbf{Q}}_L(\tau)$ and $\hat{\mathbf{Q}}_R(\tau)$ are time Taylor series expansions around the initial points $\mathbf{P}_L(0_+)$ and $\mathbf{P}_R(0_-)$, respectively, evaluated at $\tau$. These expansions become

$$\left.\begin{aligned} \hat{\mathbf{Q}}_L(\tau) &= \mathbf{P}_L(0) + \textstyle\sum_{k=1}^{M} \frac{\tau^k}{k!} \mathbf{G}^{(k)} \left(\mathbf{P}_L(0), \ldots, \frac{d^k}{dx^k}\mathbf{P}_L(0)\right) \,, \\ \hat{\mathbf{Q}}_R(\tau) &= \mathbf{P}_R(0) + \textstyle\sum_{k=1}^{M} \frac{\tau^k}{k!} \mathbf{G}^{(k)} \left(\mathbf{P}_R(0), \ldots, \frac{d^k}{dx^k}\mathbf{P}_R(0)\right) \,, \end{aligned}\right\} \tag{14}$$

after applying the Cauchy–Kowalewskaya procedure. In this solution strategy, a classical Riemann problem, possibly non-linear, is solved at each required time $\tau$ and the evaluation of two Taylor series expansions at time $\tau$ are also needed.

In the next section we present our new implicit solver for the Generalized Riemann problem with stiff source terms.

## 3. The new implicit GRP solver

In this section we proposed a new solver for the GRP that is able to deal with stiff source terms. So far, the only GRP solver able to do this was the DET solver proposed by Dumbser, Enaux and Toro [13], which is by now the standard technique in ADER to solve hyperbolic balance laws with stiff source terms to high order of accuracy. Essentially, DET is an implicit, numerical version of the HEOC solver for the GRP, in which the time evolution is carried through a sophisticated numerical approach. A preliminary version of the new solver was first communicated, for the scalar case, in [31], and for second-order schemes for non-linear systems in [33]. In this paper we present the general case.

The key ingredient of the new solver is the implicit Taylor series expansion contained in the following:

**Lemma 3.1.** *Let* $\mathbf{Q}(x,\tau)$ *be an analytic function, then* $\mathbf{Q}(x,\tau)$ *can be expressed in terms of the implicit Taylor series in time*

$$\mathbf{Q}(x,\tau) = \mathbf{Q}(x,0_+) - \sum_{k=1}^{\infty} \frac{(-\tau)^k}{k!} \partial_t^{(k)} \mathbf{Q}(x,\tau) \,. \tag{15}$$

**Proof.** See [33]. □

We remark that it is the implicitness of the Taylor series that allows us to handle stiff source terms with the explicit ADER methods. The resulting solver presented here is an implicit version of the TT and HEOC solvers described above. Note that in practice we use the truncated series of $M$ terms, namely

$$\mathbf{Q}(0,\tau) = \mathbf{Q}(0,0_+) - \sum_{k=1}^{M} \frac{(-\tau)^k}{k!} \partial_t^{(k)} \mathbf{Q}(0,\tau) \,, \tag{16}$$

where the Cauchy–Kowalewskaya functionals are used to evaluate time derivatives as in (10), namely

$$\partial_t^{(k)} \mathbf{Q}(0,\tau) = \mathbf{G}^{(k)}(\mathbf{Q}(0,\tau), \ldots, \partial_x^{(k)} \mathbf{Q}(0,\tau)) \,. \tag{17}$$

Then (16) becomes

$$\mathbf{Q}(0,\tau) = \mathbf{Q}(0,0_+) - \sum_{k=1}^{M} \frac{(-\tau)^k}{k!} \mathbf{G}^{(k)}(\mathbf{Q}(0,\tau), \ldots, \partial_x^{(k)} \mathbf{Q}(0,\tau)) \,. \tag{18}$$

Recall that the numerical flux evaluated at the solution of the GRP obtained implicitly is used in the one-step explicit finite volume formula (2). Therefore the ADER scheme is globally explicit with a locally implicit solver for the GRP. In the preliminary version [31], spatial derivatives at $\tau$ were approximated by $\partial_x^{(k)} \mathbf{Q}(0,0_+)$. However, such procedure severely penalised the stability of the explicit ADER schemes and very small Courant numbers were needed to preserve stability. Subsequently, in [33], the stability range of the scheme was improved by considering the evolution of spatial derivatives also in an implicit manner. However, only second-order of accuracy was implemented. Here, we extend the idea to arbitrary order of accuracy while retaining stability, with all spatial derivatives evolved implicitly. We shall present two approaches, as seen below.

### 3.1. Reduced implicit Taylor expansion approach (RITA)

As reconstruction polynomials are of degree $M$, we will assume $\partial_x^{(l)} \mathbf{Q} \equiv 0$, for $l > M$. Therefore, for evolving spatial derivatives $\partial_x^{(l)} \mathbf{Q}(0,\tau)$ for $l = 1, \ldots, M$, we only take $k$ such that $l + k = M$, hence

$$\partial_x^{(l)} \mathbf{Q}(0,\tau) = \partial_x^{(l)} \mathbf{Q}(0,0_+) - \sum_{k=1}^{M-l} \frac{(-\tau)^k}{k!} \partial_t^{(k)} (\partial_x^{(l)} \mathbf{Q}(0,\tau)) \,. \tag{19}$$

By using the Cauchy–Kowalewskaya procedure, (19) becomes

$$\partial_x^{(l)} \mathbf{Q}(0,\tau) = \partial_x^{(l)} \mathbf{Q}(0,0_+) - \sum_{k=1}^{M-l} \frac{(-\tau)^k}{k!} \partial_x^{(l)} \mathbf{G}^{(k)}(\mathbf{Q}(0,\tau), \ldots, \partial_x^{(k)} \mathbf{Q}(0,\tau)) \,. \tag{20}$$

Note that (18) and (20) form a system of algebraic non-linear equations for $\mathbf{U} = [\mathbf{U}_0, \ldots, \mathbf{U}_M]^T$, with $\mathbf{U}_l = \partial_x^{(l)} \mathbf{Q}(0,\tau)$, which can be written as

$$\left.\begin{aligned}
\mathbf{U}_0 &= \mathbf{Q}(0,0_+) - \sum_{l=1}^{M} \frac{(-\tau)^l}{l!} \mathbf{G}^{(l)}(\mathbf{U}_0, \ldots, \mathbf{U}_l) \,, \\
\mathbf{U}_1 &= \partial_x \mathbf{Q}(0,0_+) - \sum_{k=1}^{M-1} \frac{(-\tau)^k}{k!} \mathbf{D}^{(k+l)}(\mathbf{U}_0, \ldots, \mathbf{U}_{l+k}) \,, \\
&\vdots \\
\mathbf{U}_l &= \partial_x^{(l)} \mathbf{Q}(0,0_+) - \sum_{k=1}^{M-l} \frac{(-\tau)^k}{k!} \mathbf{D}^{(k+l)}(\mathbf{U}_0, \ldots, \mathbf{U}_{l+k}) \,, \\
&\vdots \\
\mathbf{U}_M &= \partial_x^{(M)} \mathbf{Q}(0,0_+) \,.
\end{aligned}\right\} \tag{21}$$

Here $\mathbf{D}^{(k+l)}$ is a functional satisfying $\partial_x^{(l)}\mathbf{G}^{(k)}(\mathbf{Q},\ldots,\partial_x^{(k)}\mathbf{Q}) := \mathbf{D}^{(k+l)}(\mathbf{Q},\ldots,\partial_x^{(k+l)}\mathbf{Q})$. A closed form for $\mathbf{D}^{(k+l)}$ can be obtained by using symbolic manipulators. Now, the problem to solve is the following: find $\mathbf{U}^*$ such that

$$\mathbf{L}(\mathbf{U}^*) = \mathbf{U}^* - \mathbf{H}_{RITA}(\mathbf{U}^*) = \mathbf{0}\,, \tag{22}$$

where

$$\mathbf{H}_{RITA}(\mathbf{U}) = \begin{bmatrix} \mathbf{Q}(0,0_+) - \displaystyle\sum_{l=1}^{M} \frac{(-\tau)^l}{l!}\mathbf{G}^{(l)}(\mathbf{U}_0,\ldots,\mathbf{U}_l) \\ \vdots \\ \partial_x^{(l)}\mathbf{Q}(0,0_+) - \displaystyle\sum_{k=1}^{M-l} \frac{(-\tau)^k}{k!}\mathbf{D}^{(k+l)}(\mathbf{U}_0,\ldots,\mathbf{U}_{k+l}) \\ \vdots \\ \partial_x^{(M)}\mathbf{Q}(0,0_+) \end{bmatrix}. \tag{23}$$

In the next section we present a variation of the technique.

### 3.2. Complete implicit Taylor expansion approach (CITA)

Here, we use implicit Taylor series with $M$ terms for all spatial derivatives and, taking $\partial_x^{(l)}\mathbf{Q} \equiv \mathbf{0}$, for $l > M$, we obtain

$$\partial_x^{(l)}\mathbf{Q}(0,\tau) = \partial_x^{(l)}\mathbf{Q}(0,0_+) - \sum_{k=1}^{M} \frac{(-\tau)^k}{k!}\partial_x^{(l)}\mathbf{G}^{(k)}(\mathbf{Q}(0,\tau),\ldots,\partial_x^{(k)}\mathbf{Q}(0,\tau))\,. \tag{24}$$

Again we end up with non-linear algebraic system formed by (18) and (24) for $\mathbf{U} = [\mathbf{U}_0,\mathbf{U}_1,\ldots,\mathbf{U}_M]^T$, namely

$$\left.\begin{aligned} \mathbf{U}_0 &= \mathbf{Q}(0,0_+) - \sum_{l=1}^{M} \frac{(-\tau)^l}{l!}\mathbf{G}^{(l)}(\mathbf{U}_0,\ldots,\mathbf{U}_l)\,, \\ \mathbf{U}_1 &= \partial_x\mathbf{Q}(0,0_+) - \sum_{k=1}^{M} \frac{(-\tau)^k}{k!}\mathbf{D}^{(k+1)}(\mathbf{U}_0,\ldots,\mathbf{U}_{k+1})\,, \\ &\vdots \\ \mathbf{U}_l &= \partial_x^{(l)}\mathbf{Q}(0,0_+) - \sum_{k=1}^{M} \frac{(-\tau)^k}{k!}\mathbf{D}^{(k+l)}(\mathbf{U}_0,\ldots,\mathbf{U}_{k+l})\,, \\ &\vdots \\ \mathbf{U}_M &= \partial_x^{(M)}\mathbf{Q}(0,0_+) - \sum_{k=1}^{M} \frac{(-\tau)^k}{k!}\mathbf{D}^{(k+M)}(\mathbf{U}_0,\ldots,\mathbf{U}_{k+M})\,. \end{aligned}\right\} \tag{25}$$

Note that $\partial_x^{(r)}\mathbf{Q} = \mathbf{0}$ for all $r > M$. Therefore, the problem is: find the root $\mathbf{U}^*$ of

$$\mathbf{L}(\mathbf{U}^*) = \mathbf{U}^* - \mathbf{H}_{CITA}(\mathbf{U}^*) = \mathbf{0}\,, \tag{26}$$

where

$$\mathbf{H}_{CITA}(\mathbf{U}) = \begin{bmatrix} \mathbf{Q}(0,0_+) - \displaystyle\sum_{l=1}^{M} \frac{(-\tau)^l}{l!}\mathbf{G}^{(l)}(\mathbf{U}_0,\ldots,\mathbf{U}_l) \\ \vdots \\ \partial_x^{(l)}\mathbf{Q}(0,0_+) - \displaystyle\sum_{k=1}^{M} \frac{(-\tau)^k}{k!}\mathbf{D}^{(k+l)}(\mathbf{U}_0,\ldots,\mathbf{U}_{k+l}) \\ \vdots \\ \partial_x^{(M)}\mathbf{Q}(0,0_+) - \displaystyle\sum_{k=1}^{M} \frac{(-\tau)^k}{k!}\mathbf{D}^{(k+M)}(\mathbf{U}_0,\mathbf{0}\ldots,\mathbf{0}) \end{bmatrix}. \tag{27}$$

In this paper, we adopt the Newton reduced-step method to solve these non-linear algebraic systems. However, standard fixed-point iteration procedures can be used to find the roots of (22) and (26). See Appendix B for a comparison between the standard Newton and Newton reduced-step methods. For both approaches the sought solution of the GRP is $\mathbf{Q}(0,\tau)=\mathbf{U}_0^*$.

Note that the presented implicit methodology is applicable in both the TT and HEOC explicit frameworks. For the TT framework the leading term $\mathbf{Q}(0,0_+)$ and spatial derivatives $\partial_x^{(k)}\mathbf{Q}(0,0_+)$ are calculated right at the interface. For the HEOC framework, two algebraic systems are first solved on each side of the interface to account for data evolution. For each evolved quantity $\mathbf{U}_k$, for $k=0,\ldots,M$, we require a leading term on each side, which are given by $\mathbf{P}_L(0_+)$ and $\mathbf{P}_R(0_-)$. In the final step to calculate the GRP solution at $t=\tau$ we solve a classical Riemann problem (13) and evaluate the similarity solution at the interface. Once the GRP solution as a function of time is available at the interface we compute the numerical flux by evaluating the integral (5). The numerical source $\mathbf{S}_i$ in (2) is evaluated as in (6), where the function $\mathbf{Q}_j(\tau)$ is evaluated in identically the same way as in the evolution step of the implicit version of the HEOC solver. Note that the initial condition within the cell is continuous.

## 4. Analysis and assessment of the implicit GRP solver

Here we present two theoretical results concerning our solution $q_{LR}(\tau)$ of the GRP for a model balance law with stiff source term.

### 4.1. Analysis for the scalar linear case

We study some theoretical properties of our GRP solver for the scalar linear advection–reaction equation

$$\partial_t q+\lambda\partial_x q=\beta q\,, \tag{28}$$

with $\lambda$ and $\beta\leq 0$ constant values. The stiffness of the sourceterm is characterised by $|\beta|\gg 1$.

**Proposition 4.1.** *The solution of the Generalized Riemann Problem given by the proposed methodology with the CITA variant for spatial derivatives (26) satisfies:*

A. *The algebraic system is well posed, including the stiff regime.*
B. *The solution remains bounded in the stiff regime and converges to the null function for $\tau>0$.*

**Proof.** *Proof of A.* After some algebraic manipulations the Taylor series expansions (26) can be written as

$$\sum_{j=0}^{M}\frac{(\lambda\tau)^j}{j!}\partial_x^{(j+l)}q(0,\tau)\sum_{m=0}^{M-j}\frac{(-\tau\beta)^m}{(m)!}-\partial_x^{(l)}q(0,0_+)=0\,, \tag{29}$$

with $j=0,\ldots,M$. Therefore, the Jacobian of the algebraic system (26) satisfies

$$\partial_{\mathbf{U}}\mathbf{L}_{l,l+j}=\frac{(\lambda\tau)^j}{j!}\sum_{m=0}^{M-j}\frac{(-\tau\beta)^m}{(m)!}\,, \tag{30}$$

with $j=0,\ldots,M-l$ and $l=0,\ldots,M$. The Jacobian associated with this system is an upper triangular matrix and therefore system (26) is always well posed, specially in the stiff limit, where the dominant term is

$$\sum_{m=0}^{M}\frac{(-\tau\beta)^m}{m!}\,. \tag{31}$$

*Proof of B.* Firstly we show that the solution to the Generalized Riemann Problem remains bounded and is zero when $|\beta|\to\infty$. From (30) we note that for $\tau>0$ we have

$$\frac{|\partial_{\mathbf{U}}\mathbf{L}_{l,l+j}|}{|\partial_{\mathbf{U}}\mathbf{L}_{l,l}|}\to 0\,,\ \text{as}\ |\beta|\to\infty\,, \tag{32}$$

for all $l=0,\ldots,M$ and $j=1,\ldots,M-l$. Secondly, as the solution is obtained from solving the linear system

$$(\partial_{\mathbf{U}}\mathbf{L})\mathbf{U}=[q(0,0_+),\ldots,\partial_x^{(M)}q(0,0_+)]^T \tag{33}$$

and the Jacobian matrix is an upper triangular matrix, then the solution is obtained as

$$\left.\begin{aligned} U_M &= \frac{\partial_x^{(M)} q(0,0_+)}{\sum_{m=0}^{M} \frac{(-\tau\beta)^m}{m!}}\,, \\ U_{M-1} &= \frac{\partial_x^{(M-1)} q(0,0_+) - \partial_{\mathbf{U}}\mathbf{L}_{M-1,M} U_M}{\partial_{\mathbf{U}}\mathbf{L}_{M-1,M-1}}\,, \\ U_k &= \frac{\partial_x^{(k)} q(0,0_+) - \sum_{j=k+1}^{M} \partial_{\mathbf{U}}\mathbf{L}_{k,j} U_j}{\partial_{\mathbf{U}}\mathbf{L}_{k,k}}\,, \end{aligned}\right\} \tag{34}$$

with $k = M-1, M-2, \ldots, 0$. Therefore, from the ratio (32) we obtain $U_k \to 0$ when $|\beta| \to \infty$ and $\tau > 0$. On the other hand, from the Cauchy–Kowalewskaya procedure

$$\partial_t^{(k)} q(0,\tau) = G^{(k)}(q(0,\tau), \ldots, \partial_x^{(k)} q(0,\tau)) = 0\,, \tag{35}$$

with $k = 0, \ldots, M$. Therefore, $q(0,\tau) \equiv 0$. That is, in the stiff regime the solution is identically the null function as claimed. □

**Proposition 4.2.** *The solution of the Generalized Riemann Problem given by the proposed methodology with the RITA variant for spatial derivatives satisfies:*

A. *The algebraic system is well posed, including in the stiff regime.*
B. *The solution remains bounded in the stiff regime and tends to zero for $\tau > 0$.*

**Proof.** *Proof of A.* After some algebraic manipulations the Taylor series expansions for spatial derivatives become

$$\sum_{j=0}^{M-l} \frac{(\lambda\tau)^j}{j!} \partial_x^{(j+l)} q(0,\tau) \sum_{m=0}^{M-j} \frac{(-\tau\beta)^m}{(m)!} - \partial_x^{(l)} q(0,0_+) = 0\,, \tag{36}$$

with $j = 0, \ldots, M$. Thus the Jacobian associated to the algebraic system (22) satisfies that

$$\partial_{\mathbf{U}}\mathbf{L}_{l,l+j} = \frac{(\lambda\tau)^j}{j!} \sum_{m=0}^{M-l-j} \frac{(-\tau\beta)^m}{(m)!}\,, \tag{37}$$

with $j = 0, \ldots, M-l$ and $l = 0, \ldots, M$. Then, the Jacobian is an upper triangular matrix. Therefore, system (22) is always well posed, specially in the stiff limit, as claimed.

*Proof of B.* The solution is directly obtained as follows

$$\left.\begin{aligned} U_M &= \partial_x^{(M)} q(0,0_+)\,, \\ U_{M-1} &= \frac{\partial_x^{(M-1)} q(0,0_+) - \partial_{\mathbf{U}}\mathbf{L}_{M-1,M} U_M}{\partial_{\mathbf{U}}\mathbf{L}_{M-1,M-1}}\,, \\ U_k &= \frac{\partial_x^{(k)} q(0,0_+) - \sum_{j=k+1}^{M} \partial_{\mathbf{U}}\mathbf{L}_{k,j} U_j}{\partial_{\mathbf{U}}\mathbf{L}_{k,k}}\,, \end{aligned}\right\} \tag{38}$$

with $k = M-1, M-2, \ldots, 0$. On the other hand, from (37) we observe that for $\tau > 0$ we have

$$\frac{|\partial_{\mathbf{U}}\mathbf{L}_{l,l+j}|}{|\partial_{\mathbf{U}}\mathbf{L}_{l,l}|} \to 0\,, \text{ as } |\beta| \to \infty\,, \tag{39}$$

for all $l < M$ and $j = 1, \ldots, M-l$. Therefore, from (38) we obtain $U_k \to 0$ for $k < M$, when $|\beta| \to \infty$. □

### 4.2. Assessment of the new generalized Riemann solver

Here we assess the reformulation of the HEOC solver in combination with RITA and CITA approaches for evolving the spatial derivatives. We are only interested in the solution $q_{LR}(\tau)$ to the GRP (4) along the $t$-axis, that is the interface position $x = 0$, as function of time. If an exact solution for the GRP is not available, a reference solution can be obtained by following the strategy proposed in [8,30]. In what follows we adopt a convention to denote the combination of the GRP solver strategy and the evolution for spatial derivatives. For example *MT-HEOC-RITA* means that the implicit formulation of the HEOC solver is combined with the RITA approach for evolving spatial derivatives.

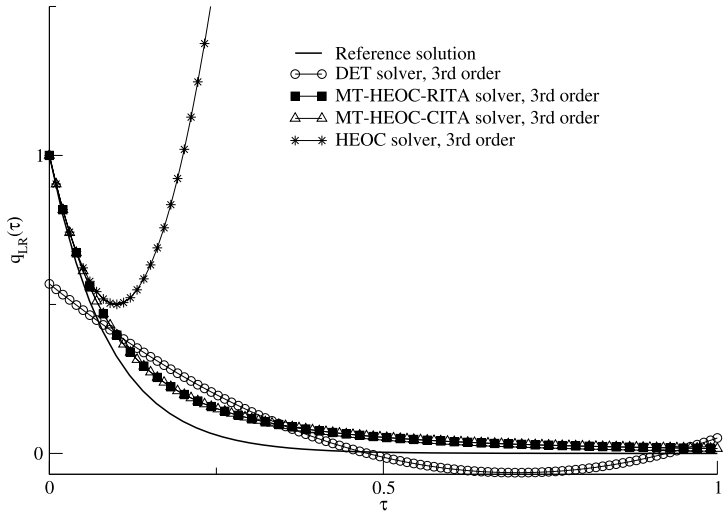


**Fig. 1.** GRP solutions for the linear advection–reaction equation. Comparison between the exact solution (full line) and approximate solutions of third order obtained from the present solvers MT-HEOC-RITA and MT-HEOC-CITA. For comparison we also display the conventional *explicit* HEOC solver (stars) and the approximate implicit solution from the DET solver (circles). Parameters: $\lambda = 1$, $\beta = -10$.

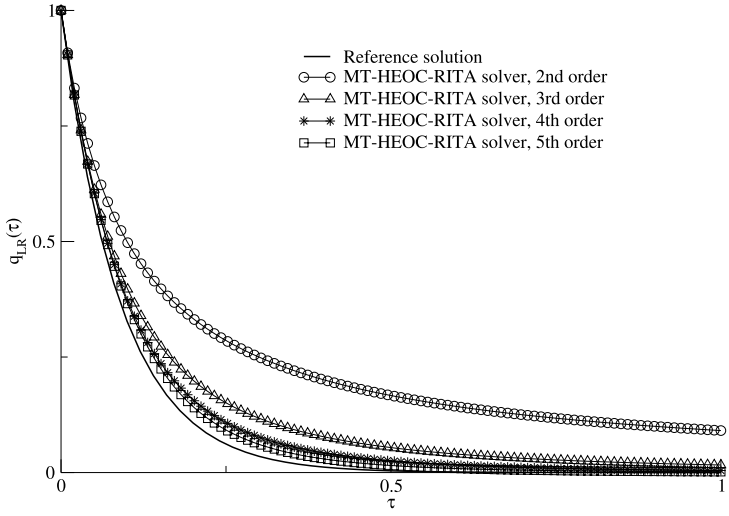


**Fig. 2.** GRP solutions for the linear advection–reaction equation. Comparison between the exact solution (full line) and the approximations obtained from MT-HEOC-RITA of several orders of accuracy: 2nd (circles), 3rd (triangles), 4th (stars) and 5th (squares). Parameters: $\lambda = 1$ and $\beta = -10$.

### *4.3. The GRP for the linear advection–reaction equation*

We first apply the methodology to solve the simplest linear scalar model, (28) with a constant initial condition

$$q(x, 0) = 1 \,, \tag{40}$$

whose exact solution at the interface is $q_{LR}(\tau) = e^{\beta\tau}$.

Fig. 1 shows a comparison between the exact solution (full line) and approximate solutions from the present solvers MT-HEOC-RITA (filled squares) and MT-HEOC-CITA (triangles). For comparison we also display the conventional *explicit* HEOC solver (stars) and the approximate implicit solution from the DET solver (circles). Clearly, and as expected, the explicit GRP solver is unsuitable. The present implicit solutions compare fairly with the conventional implicit DET solution. Fig. 2 shows the exact solution (full line) compared to GRP solutions obtained with the MT-HEOC-RITA solver for 2nd (circles), 3rd (triangles), 4th (stars) and 5th (squares) orders of accuracy. The approximations improve as the order of accuracy increases, as expected. Table 1 displays errors in three norms, namely $L_\infty$, $L_1$ and $L_2$, of various solvers at time $\tau_{out} = 1$, for $\lambda = 1$ and $\beta = -10$. As noted earlier, the explicit formulation shown in the last column is unsuitable, whereas the implicit solvers provide acceptable approximations, noting that both reformulations presented in this paper provide similar results and show smaller errors than those from the existing implicit DET solver, at least for this test problem.

**Table 1**
Errors in GRP solutions for the linear advection–reaction with $\lambda = 1$ and $\beta = -10$. Absolute errors in $L_\infty$, $L_1$ and $L_2$ norms, up to $\tau_{out} = 1$, for solvers of 3rd, 4th and 5th orders of accuracy.

| | DET solver | MT-RITA-HEOC solver | MT-CITA-HEOC solver | HEOC solver |
|---|---|---|---|---|
| $\mathcal{O}_3$ | | | | |
| $L_\infty$-error | 4.310e−01 | 9.239e−02 | 9.239e−02 | 4.100e+01 |
| $L_1$-error | 7.261e−02 | 4.858e−02 | 4.858e−02 | 1.266e+01 |
| $L_2$-error | 9.859e−02 | 5.513e−02 | 5.513e−02 | 1.769e+01 |
| $\mathcal{O}_4$ | | | | |
| $L_\infty$-error | 2.291e−01 | 5.112e−02 | 5.112e−02 | 1.257e+02 |
| $L_1$-error | 4.051e−02 | 2.372e−02 | 2.372e−02 | 2.943e+01 |
| $L_2$-error | 5.540e−02 | 2.872e−02 | 2.872e−02 | 4.627e+01 |
| $\mathcal{O}_5$ | | | | |
| $L_\infty$-error | 1.043e−01 | 4.121e−02 | 4.121e−02 | 2.910e+02 |
| $L_1$-error | 1.995e−02 | 1.550e−02 | 1.550e−02 | 5.517e+01 |
| $L_2$-error | 2.970e−02 | 2.034e−02 | 2.034e−02 | 9.530e+01 |

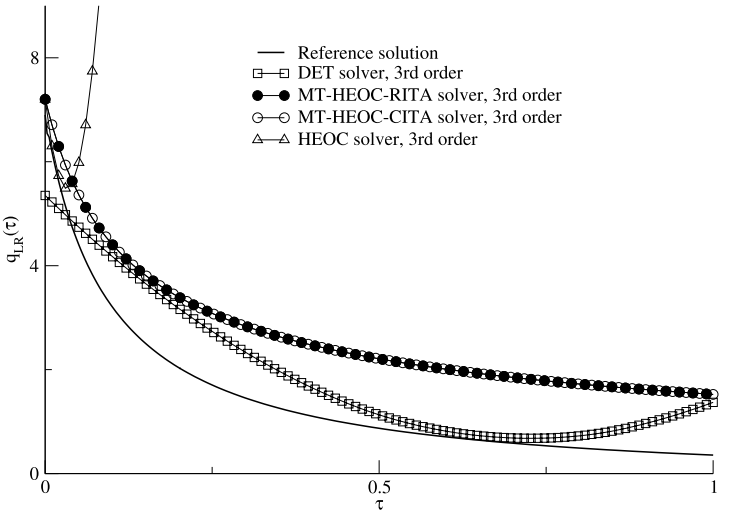


**Fig. 3.** GRP solutions for Burgers' equation with a quadratic source term. Comparison between the reference solution (full line) and approximate GRP solutions of third order: DET solver (square), MT-HEOC-RITA solver (black circles), MT-HEOC-CITA solver (white circles), HEOC solver (triangles). $\beta = -1$.

### 4.4. The GRP for Burgers equation with a quadratic source term

Here we consider the GRP for the Burgers equation with a quadratic source term, given by

$$\left.\begin{aligned} &\partial_t q(x,t) + \partial_x\left(\frac{q(x,t)^2}{2}\right) = \beta q(x,t)^2\,, \\ &q(x,0) = \begin{cases} p_L(x) \equiv 7.9 + x + \frac{1}{2}x^2, & x < 0\,, \\ p_R(x) \equiv 3.2 - \frac{1}{2}x - \frac{3}{10}x^2, & x > 0\,, \end{cases} \end{aligned}\right\} \tag{41}$$

with $\beta \leq 0$ a constant value.

Fig. 3 shows comparisons of approximations with the exact solution. As expected, the conventional explicit solver only works for very small times. Fig. 4 shows the results from the MT-HEOC-RITA solver of orders 2nd (left triangles), 3rd (squares), 4th (circles) and 5th (up triangles). As expected, the accuracy of the approximation is improved as the order of solvers increases. Table 2 shows absolute errors in the three norms $L_\infty$, $L_1$ and $L_2$, for $\tau_{out} = 1$ for $\beta = -1$. We observe that in this stiff regime the present implicit solvers and the DET solver work very well. The present implicit solvers give visibly different results, unlike the linear case.

### 4.5. The GRP for a system of non-linear balance laws

Let us consider the Generalized Riemann Problem for a model inhomogeneous non-linear system, namely

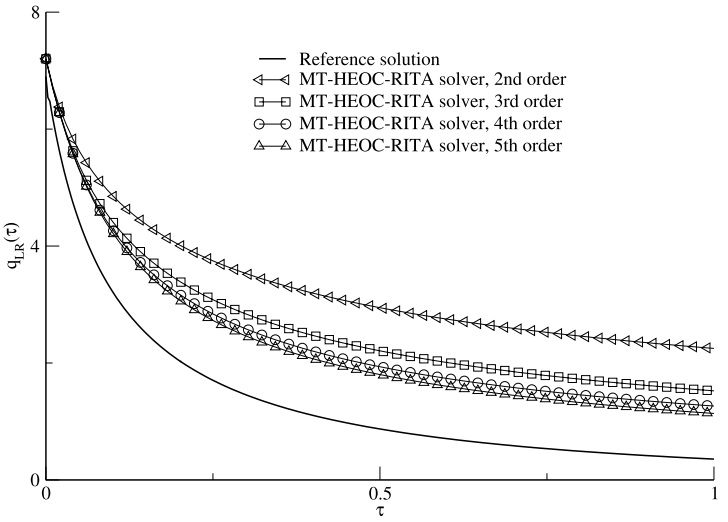


**Fig. 4.** GRP solutions for Burgers' equation with a quadratic source term. Comparison between the reference solution (full line) and approximate solutions from the MT-HEOC-RITA solver for 2nd (left triangles), 3rd (squares), 4th (circles) and 5th (up triangles) orders. $\beta = -1$.

**Table 2**
Burgers' equation with $\beta = -1$. Relative errors in $L_\infty$, $L_1$ and $L_2$ norms, up to $\tau_{out} = 1$, for solvers of 3rd, 4th and 5th order of accuracy.

| | DET solver | MT-RITA-HEOC solver | MT-CITA-HEOC solver | HEOC solver |
|---|---|---|---|---|
| $\mathcal{O}_3$ | | | | |
| $L_\infty$-error | 4.334e+00 | 3.273e+00 | 3.273e+00 | 4.056e+03 |
| $L_1$-error | 1.128e+00 | 1.583e+00 | 1.583e+00 | 9.247e+02 |
| $L_2$-error | 1.465e+00 | 1.828e+00 | 1.828e+00 | 1.457e+03 |
| $\mathcal{O}_4$ | | | | |
| $L_\infty$-error | 5.425e+00 | 2.545e+00 | 4.947e+00 | 2.158e+04 |
| $L_1$-error | 1.966e+00 | 1.255e+00 | 1.701e+00 | 4.019e+03 |
| $L_2$-error | 2.743e+00 | 1.437e+00 | 2.209e+00 | 6.955e+03 |
| $\mathcal{O}_5$ | | | | |
| $L_\infty$-error | 1.113e+00 | 2.189e+00 | 6.532e+00 | 9.805e+05 |
| $L_1$-error | 5.525e−01 | 1.097e+00 | 2.196e+00 | 1.549e+05 |
| $L_2$-error | 6.857e−01 | 1.247e+00 | 3.003e+00 | 2.898e+05 |

$$\left.\begin{aligned} &\partial_t \mathbf{Q}(x,t) + \partial_x \mathbf{F}(\mathbf{Q}(x,t)) = \mathbf{S}(\mathbf{Q}(x,t)) \,, \\ &\mathbf{Q}(x,0) = \begin{cases} \mathbf{P}_L(x), & x < 0 \,, \\ \mathbf{P}_R(x), & x < 0 \,, \end{cases} \end{aligned}\right\} \tag{42}$$

with $\mathbf{Q} = [u, v]^T$ and

$$\left.\begin{aligned} \mathbf{F}(\mathbf{Q}) = \begin{bmatrix} \frac{1}{9}\left(\frac{5}{2}u^2 + v^2 - uv\right) \\ \frac{1}{9}\left(4uv - u^2 + \frac{1}{2}v^2\right) \end{bmatrix} \,, \quad \mathbf{S}(\mathbf{Q}) = \begin{bmatrix} \beta\left(\frac{2u-v}{3}\right)^2 \\ -\beta\left(\frac{2u-v}{3}\right)^2 \end{bmatrix} \,, \end{aligned}\right\} \tag{43}$$

where $\beta \leq 0$ is a constant value. As initial condition we take polynomial distributions

$$\mathbf{P}_L(x) = \begin{bmatrix} 4 - \frac{1}{5}x + x^2 \\ 2 + x + \frac{3}{10}x^2 \end{bmatrix} \,, \quad \mathbf{P}_R(x) = \begin{bmatrix} 4 + \frac{1}{50}x + \frac{1}{2}x^2 \\ 2 + 2x + 2x^2 \end{bmatrix} \,. \tag{44}$$

Figs. 5 and 6 show results of third order solvers for variables $u$ and $v$, respectively. The present implicit solvers compare well with the exact solution and the DET solver, though they exhibit slightly different behaviours. The conventional explicit HEOC solver is unsuitable. Tables 3 and 4 show errors for times up to $\tau_{out} = 0.3$ and $t_{out} = 0.45$ respectively. For small times all GRP solutions remain accurate, though the DET solver and the present implicit reformulations of HEOC prove the best approximations. The same remarks apply to results of Table 4.

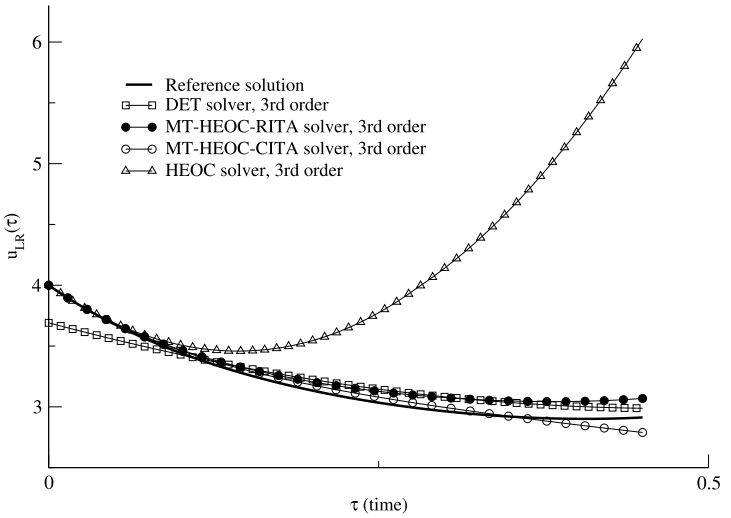


**Fig. 5.** GRP solution for variable $u$ for the model non-linear system. Comparison between the reference solution (full line) and approximate solutions of third order accuracy: DET solver (square), MT-HEOC-RITA solver (black circles), MT-HEOC-CITA solver (white circles) and HEOC solver (triangles). Parameter: $\beta = -2$.

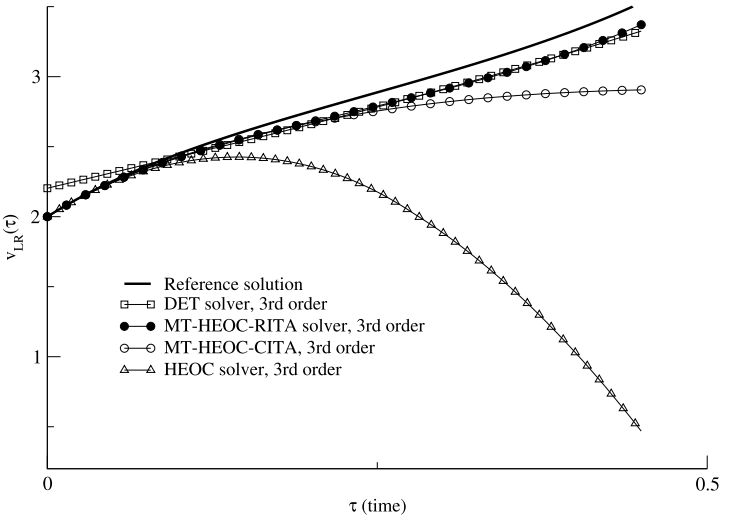


**Fig. 6.** GRP solution for variable $v$ for the model non-linear system. Comparison between the reference solution (full line) and approximate solutions of third order accuracy: DET solver (square), MT-HEOC-RITA solver (black circles), MT-HEOC-CITA solver (white circles) and HEOC solver (triangles). Parameter: $\beta = -2$.

In this section we have assessed the quality of the approximate solutions of the Generalized Riemann Problem at $x = 0$ (along the $t$-axis), as a function of time. In next section we apply these GRP solvers locally, in the frame of ADER schemes, to solve the general initial boundary value problem. The resulting ADER schemes will remain globally explicit and the time step will be computed through the conventional CFL condition, with CFL numbers close to unity, even for very stiff problems.

## 5. Assessment of the new GRP solver in the context of ADER schemes

We first select test problems with stiff source terms and carry out a systematic convergence rate study to assess the accuracy of the explicit ADER methods with implicit GRP solvers. Schemes of up to 5th order of accuracy in space and time are implemented. We also assess the schemes for solving a scalar problem with a stiff non-linear source term and a shock wave.

### *5.1. The linear advection–reaction equation*

Here we consider the IBVP for the linear advection–reaction equation

**Table 3**
GRP solution errors in $L_\infty$, $L_1$ and $L_2$ norms, computed up to $\tau_{out} = 0.3$, for solvers of 3rd, 4th and 5th orders of accuracy.

| | DET solver | MT-RITA-HEOC solver | MT-CITA-HEOC solver | HEOC solver |
|---|---|---|---|---|
| $\mathcal{O}_3$ | | | | |
| $L_\infty$- error $u$ | 7.725e−02 | 3.843e−02 | 1.523e−02 | 8.343e−01 |
| $L_\infty$- error $v$ | 1.017e−01 | 3.905e−02 | 7.075e−02 | 7.064e−01 |
| $\sqrt{u^2+v^2}$ | 1.277e−01 | 5.479e−02 | 7.237e−02 | 1.093e+00 |
| $L_1$-error $u$ | 3.190e−02 | 1.648e−02 | 8.691e−03 | 2.368e−01 |
| $L_1$-error $v$ | 3.439e−02 | 1.933e−02 | 2.412e−02 | 2.227e−01 |
| $\sqrt{u^2+v^2}$ | 4.691e−02 | 2.540e−02 | 2.564e−02 | 3.251e−01 |
| $L_2$-error $u$ | 3.535e−02 | 2.085e−02 | 1.028e−02 | 3.446e−01 |
| $L_2$-error $v$ | 3.837e−02 | 2.344e−02 | 3.231e−02 | 3.112e−01 |
| $\sqrt{u^2+v^2}$ | 5.217e−02 | 3.137e−02 | 3.390e−02 | 4.643e−01 |
| $\mathcal{O}_4$ | | | | |
| $L_\infty$-error $u$ | 3.298e−02 | 1.622e−02 | 5.021e−01 | 6.385e−01 |
| $L_\infty$-error $v$ | 3.347e−02 | 1.742e−02 | 1.019e+00 | 4.177e−01 |
| $\sqrt{u^2+v^2}$ | 4.699e−02 | 2.380e−02 | 1.136e+00 | 7.630e−01 |
| $L_1$-error $u$ | 1.243e−02 | 6.026e−03 | 2.793e−02 | 1.743e−01 |
| $L_1$-error $v$ | 1.407e−02 | 7.555e−03 | 5.671e−02 | 1.458e−01 |
| $\sqrt{u^2+v^2}$ | 1.878e−02 | 9.664e−03 | 6.322e−02 | 2.273e−01 |
| $L_2$-error $u$ | 1.561e−02 | 8.059e−03 | 1.074e−01 | 2.578e−01 |
| $L_2$-error $v$ | 1.546e−02 | 9.585e−03 | 2.184e−01 | 2.040e−01 |
| $\sqrt{u^2+v^2}$ | 2.197e−02 | 1.252e−02 | 2.433e−01 | 3.287e−01 |
| $\mathcal{O}_5$ | | | | |
| $L_\infty$-error $u$ | 5.497e−02 | 6.809e−03 | 8.192e−03 | 1.661e+00 |
| $L_\infty$-error $v$ | 2.756e−01 | 8.252e−03 | 3.089e−02 | 1.390e+00 |
| $\sqrt{u^2+v^2}$ | 2.810e−01 | 1.070e−02 | 3.196e−02 | 2.166e+00 |
| $L_1$-error $u$ | 2.518e−02 | 2.159e−03 | 1.270e−03 | 3.157e−01 |
| $L_1$-error $v$ | 4.403e−02 | 3.285e−03 | 6.894e−03 | 2.909e−01 |
| $\sqrt{u^2+v^2}$ | 5.072e−02 | 3.931e−03 | 7.010e−03 | 4.292e−01 |
| $L_2$-error $u$ | 3.054e−02 | 3.064e−03 | 2.430e−03 | 5.463e−01 |
| $L_2$-error $v$ | 6.484e−02 | 4.256e−03 | 1.119e−02 | 4.844e−01 |
| $\sqrt{u^2+v^2}$ | 7.167e−02 | 5.244e−03 | 1.145e−02 | 7.301e−01 |

$$\left.\begin{aligned} \partial_t q(x,t) + \lambda \partial_x q(x,t) = \beta q(x,t)\,, \quad x \in [0,1]\,, \\ q(x,0) = \sin(2\pi x)\,. \end{aligned}\right\} \tag{45}$$

We take $\lambda = 1$, $\beta = -10$, $C_{cfl} = 0.9$, $t_{out} = 1$ and periodic boundary conditions. Table 5 shows results for the ADER schemes using the MT-HEOC-RITA solver and Table 6 shows the corresponding results for the MT-HEOC-CITA solver. The expected theoretical orders of accuracy are reached and errors in all three norms are quite similar, for both resulting ADER methods.

Tables 7 and 8 show the results for the very stiff case with $\beta = -10\,000$, solved with the MT-HEOC-RITA and MT-HEOC-CITA solvers. We observe that in this case the convergence rate assessment overestimates the convergence rate. In what follows we provide an explanation for this phenomenon.

**Remark 1.** Notice that in general, the error $E$, which is involved in the approximation to the exact solution with a mesh of size $\Delta x$, satisfies

$$E \leq C \Delta x^p\,, \tag{46}$$

with $p$ the convergence rate and $C$ a constant, which is independent of both the mesh and the order of accuracy. To estimate $p$ through an empirical convergence rate assessment, it is assumed that

$$E \approx C \Delta x^p\,. \tag{47}$$

Assume that for a sequence of meshes of sizes $\Delta x_i$ there is an associated sequence of errors $E_i$ satisfying (47). Then we obtain

$$\frac{E_i}{E_{i+1}} = \left(\frac{\Delta x_i}{\Delta x_{i+1}}\right)^p\,. \tag{48}$$

Thus, if we take $\Delta x_i = 2\Delta x_{i+1}$, then

$$\frac{E_i}{E_{i+1}} = 2^p\,, \tag{49}$$

**Table 4**
GRP solution errors in $L_\infty$, $L_1$ and $L_2$ norms, computed up to $\tau_{out} = 0.45$, for solvers of 3rd, 4th and 5th orders of accuracy.

| | DET solver | MT-RITA-HEOC solver | MT-CITA-HEOC solver | HEOC solver |
|---|---|---|---|---|
| $\mathcal{O}_3$ | | | | |
| $L_\infty$-error $u$ | 7.725e−02 | 5.252e−02 | 3.396e−02 | 1.069e+00 |
| $L_\infty$-error $v$ | 1.017e−01 | 4.449e−02 | 1.629e−01 | 8.672e−01 |
| $\sqrt{u^2+v^2}$ | 1.277e−01 | 6.883e−02 | 1.664e−01 | 1.376e+00 |
| $L_1$-error $u$ | 1.442e−02 | 1.138e−02 | 4.481e−03 | 1.406e−01 |
| $L_1$-error $v$ | 1.642e−02 | 1.177e−02 | 2.309e−02 | 1.272e−01 |
| $\sqrt{u^2+v^2}$ | 2.186e−02 | 1.637e−02 | 2.352e−02 | 1.896e−01 |
| $L_2$-error $u$ | 2.352e−02 | 2.067e−02 | 8.423e−03 | 3.014e−01 |
| $L_2$-error $v$ | 2.691e−02 | 2.039e−02 | 4.737e−02 | 2.615e−01 |
| $\sqrt{u^2+v^2}$ | 3.574e−02 | 2.903e−02 | 4.811e−02 | 3.990e−01 |
| $\mathcal{O}_4$ | | | | |
| $L_\infty$-error $u$ | 4.055e−02 | 2.493e−02 | 7.332e−01 | 9.098e−01 |
| $L_\infty$-error $v$ | 5.057e−02 | 2.136e−02 | 1.336e+00 | 5.228e−01 |
| $\sqrt{u^2+v^2}$ | 6.482e−02 | 3.283e−02 | 1.524e+00 | 1.049e+00 |
| $L_1$-error $u$ | 6.764e−03 | 4.703e−03 | 3.281e−02 | 1.069e−01 |
| $L_1$-error $v$ | 7.677e−03 | 5.033e−03 | 6.347e−02 | 8.115e−02 |
| $\sqrt{u^2+v^2}$ | 1.023e−02 | 6.889e−03 | 7.144e−02 | 1.342e−01 |
| $L_2$-error $u$ | 1.272e−02 | 8.981e−03 | 1.163e−01 | 2.352e−01 |
| $L_2$-error $v$ | 1.342e−02 | 9.058e−03 | 2.226e−01 | 1.650e−01 |
| $\sqrt{u^2+v^2}$ | 1.849e−02 | 1.276e−02 | 2.512e−01 | 2.873e−01 |
| $\mathcal{O}_5$ | | | | |
| $L_\infty$-error $u$ | 5.497e−02 | 1.242e−02 | 5.345e−02 | 2.619e+00 |
| $L_\infty$-error $v$ | 2.756e−01 | 1.087e−02 | 1.137e−01 | 2.061e+00 |
| $\sqrt{u^2+v^2}$ | 2.810e−01 | 1.650e−02 | 1.256e−01 | 3.333e+00 |
| $L_1$-error $u$ | 1.078e−02 | 1.992e−03 | 3.996e−03 | 2.274e−01 |
| $L_1$-error $v$ | 1.814e−02 | 2.353e−03 | 1.177e−02 | 1.983e−01 |
| $\sqrt{u^2+v^2}$ | 2.110e−02 | 3.083e−03 | 1.243e−02 | 3.017e−01 |
| $L_2$-error $u$ | 1.966e−02 | 4.041e−03 | 1.136e−02 | 5.814e−01 |
| $L_2$-error $v$ | 4.148e−02 | 4.343e−03 | 2.858e−02 | 4.858e−01 |
| $\sqrt{u^2+v^2}$ | 4.590e−02 | 5.932e−03 | 3.075e−02 | 7.577e−01 |

**Table 5**
Empirical convergence rates for ADER MT-HEOC-RITA schemes, for the linear advection–reaction equation. Parameters are: $\lambda = 1$, $\beta = -10$, output time $t_{out} = 1$ and $C_{cfl} = 0.9$.

| Mesh | $L_\infty$-err | $L_\infty$-ord | $L_1$-err | $L_1$-ord | $L_2$-err | $L_2$-ord |
|---|---|---|---|---|---|---|
| Theoretical order: 2 | | | | | | |
| 32 | 2.64e−05 | 3.63 | 1.31e−05 | 3.53 | 1.48e−05 | 3.60 |
| 64 | 5.16e−06 | 2.36 | 2.84e−06 | 2.21 | 2.97e−06 | 2.31 |
| 128 | 8.05e−07 | 2.68 | 6.43e−07 | 2.14 | 6.61e−07 | 2.17 |
| 256 | 2.05e−07 | 1.98 | 1.56e−07 | 2.04 | 1.63e−07 | 2.02 |
| Theoretical order: 3 | | | | | | |
| 32 | 8.83e−07 | 2.82 | 5.61e−07 | 2.86 | 6.25e−07 | 2.85 |
| 64 | 1.20e−07 | 2.88 | 7.66e−08 | 2.87 | 8.51e−08 | 2.88 |
| 128 | 1.57e−08 | 2.94 | 1.00e−08 | 2.94 | 1.11e−08 | 2.94 |
| 256 | 2.01e−09 | 2.97 | 1.28e−09 | 2.97 | 1.42e−09 | 2.97 |
| Theoretical order: 4 | | | | | | |
| 32 | 6.23e−08 | 3.85 | 3.03e−08 | 4.01 | 3.64e−08 | 3.94 |
| 64 | 4.20e−09 | 3.89 | 1.97e−09 | 3.94 | 2.39e−09 | 3.93 |
| 128 | 2.87e−010 | 3.87 | 1.27e−010 | 3.96 | 1.54e−010 | 3.96 |
| 256 | 1.96e−011 | 3.87 | 8.13e−012 | 3.97 | 9.85e−012 | 3.97 |
| Theoretical order: 5 | | | | | | |
| 32 | 2.64e−09 | 4.97 | 1.69e−09 | 4.96 | 1.87e−09 | 4.97 |
| 64 | 8.43e−011 | 4.97 | 5.37e−011 | 4.97 | 5.96e−011 | 4.97 |
| 128 | 2.65e−012 | 4.99 | 1.69e−012 | 4.99 | 1.87e−012 | 4.99 |
| 256 | 8.30e−014 | 4.99 | 5.29e−014 | 4.99 | 5.87e−014 | 4.99 |

**Table 6**
Empirical convergence rates for ADER MT-HEOC-CITA schemes, for the linear advection–reaction equation. Parameters are: $\lambda = 1$, $\beta = -10$, output time $t_{out} = 1$ and $C_{cfl} = 0.9$.

| Mesh | $L_\infty$-err | $L_\infty$-ord | $L_1$-err | $L_1$-ord | $L_2$-err | $L_2$-ord |
|---|---|---|---|---|---|---|
| Theoretical order: 2 | | | | | | |
| 32 | 2.64e−05 | 3.63 | 1.31e−05 | 3.53 | 1.48e−05 | 3.60 |
| 64 | 5.16e−06 | 2.36 | 2.84e−06 | 2.21 | 2.97e−06 | 2.31 |
| 128 | 8.05e−07 | 2.68 | 6.43e−07 | 2.14 | 6.61e−07 | 2.17 |
| 256 | 2.05e−07 | 1.98 | 1.56e−07 | 2.04 | 1.63e−07 | 2.02 |
| Theoretical order: 3 | | | | | | |
| 32 | 5.57e−07 | 2.88 | 3.55e−07 | 2.88 | 3.94e−07 | 2.88 |
| 64 | 7.29e−08 | 2.93 | 4.64e−08 | 2.93 | 5.16e−08 | 2.94 |
| 128 | 9.29e−09 | 2.97 | 5.91e−09 | 2.97 | 6.57e−09 | 2.97 |
| 256 | 1.17e−09 | 2.99 | 7.46e−010 | 2.99 | 8.29e−010 | 2.99 |
| Theoretical order: 4 | | | | | | |
| 32 | 4.37e−08 | 3.86 | 2.18e−08 | 4.03 | 2.64e−08 | 3.94 |
| 64 | 3.01e−09 | 3.86 | 1.39e−09 | 3.97 | 1.71e−09 | 3.95 |
| 128 | 2.39e−010 | 3.65 | 8.78e−011 | 3.99 | 1.10e−010 | 3.96 |
| 256 | 2.18e−011 | 3.46 | 5.55e−012 | 3.98 | 7.06e−012 | 3.96 |
| Theoretical order: 5 | | | | | | |
| 32 | 2.08e−09 | 4.93 | 1.32e−09 | 4.97 | 1.47e−09 | 4.95 |
| 64 | 6.66e−011 | 4.96 | 4.24e−011 | 4.96 | 4.71e−011 | 4.96 |
| 128 | 2.11e−012 | 4.98 | 1.34e−012 | 4.98 | 1.49e−012 | 4.98 |
| 256 | 6.62e−014 | 4.99 | 4.22e−014 | 4.99 | 4.68e−014 | 4.99 |

which yields

$$p = \log\left(\frac{E_i}{E_{i+1}}\right) / \log(2) \, . \tag{50}$$

The conventional form to estimate the convergence rate $p$ is through (50), that is the ratio between $\log\left(\frac{E_i}{E_{i+1}}\right)$ and $\log(2)$ (assuming $\Delta x_i = 2\Delta x_{i+1}$). Now we shall see that formula (50) overestimates the correct convergence rate $p$ for the very stiff case, whose solution goes to zero.

Let us assume again that mesh size $\Delta x_1$ involves an error $E_1$ and mesh size $\Delta x_2$ involves an error $E_2$. As the exact and the numerical solutions go to zero, there exists $m_1 > 0$ such that

$$E_1 = 10^{-m_1} \Delta x_1^p \, . \tag{51}$$

Similarly, if we assume $\Delta x_1 = 2\Delta x_2$, the approximation with $\Delta x_2$ should be improved, so we can assume $E_2 < E_1$. Hence, there exists $m_2 > m_1$ such that

$$E_2 = 10^{-m_2} \Delta x_2^p \, , \tag{52}$$

so that

$$\frac{E_1}{E_2} = 10^{m_2 - m_1} 2^p \, ; \tag{53}$$

as $m_2 - m_1 > 0$, there exist $p* > 0$ such that, $10^{m_2 - m_1} = 2^{p*}$, then the convergence rate which is observed, $p$, is given by using (50), yielding

$$p^{obs} := p + p* = \log\left(\frac{E_1}{E_2}\right) / \log(2) \, . \tag{54}$$

This means that $p^{obs}$ resulting from the conventional empirical assessment is larger than the expected rate $p$

$$p \le p^{obs} \, . \tag{55}$$

This is confirmed in Tables 7 and 8, where we show the results for ADER HEOC-RITA and ADER HEOC-CITA as applied to the linear advection–reaction equation with $\beta = -10\,000$ and $t_{out} = 1$. In these tables, as the degree of mesh refinement increases, the inequality (55) is more evident, as expected.

### 5.2. A system of non-linear hyperbolic balance laws

Here we assess the high order ADER schemes with the new implicit GRP solvers as applied to a model non-linear system with stiff source terms, namely

**Table 7**
Linear advection–reaction with HEOC-RITA. Output time $t_{out} = 1$ with $C_{cfl} = 0.9$, $\lambda = 1$ and $\beta = -10\,000$. Periodic boundary conditions are applied.

| Mesh | $L_\infty$-err | $L_\infty$-ord | $L_1$-err | $L_1$-ord | $L_2$-err | $L_2$-ord | CPU |
|---|---|---|---|---|---|---|---|
| Theoretical order: 2 | | | | | | | |
| 16 | 1.27e−00 | 0.60 | 8.35e−01 | 0.37 | 8.70e−01 | 0.46 | 0.0160 |
| 32 | 9.48e−01 | 0.42 | 6.45e−01 | 0.37 | 6.57e−01 | 0.40 | 0.0400 |
| 64 | 2.39e−01 | 1.99 | 1.11e−01 | 2.54 | 1.18e−01 | 2.47 | 0.1640 |
| 128 | 1.82e−02 | 3.71 | 4.06e−03 | 4.77 | 6.50e−03 | 4.19 | 0.4200 |
| Theoretical order: 3 | | | | | | | |
| 16 | 7.64e−01 | 0.20 | 4.95e−01 | 0.31 | 5.46e−01 | 0.28 | 0.0200 |
| 32 | 3.52e−01 | 1.12 | 2.23e−01 | 1.15 | 2.49e−01 | 1.13 | 0.0360 |
| 64 | 1.06e−02 | 5.05 | 6.78e−03 | 5.04 | 7.53e−03 | 5.05 | 0.1480 |
| 128 | 5.87e−08 | 17.47 | 3.73e−08 | 17.47 | 4.15e−08 | 17.47 | 0.5880 |
| Theoretical order: 4 | | | | | | | |
| 16 | 9.12e−01 | −0.03 | 5.95e−01 | 0.08 | 6.57e−01 | 0.06 | 0.0720 |
| 32 | 5.89e−01 | 0.63 | 3.77e−01 | 0.66 | 4.18e−01 | 0.65 | 0.2760 |
| 64 | 2.76e−03 | 7.74 | 1.76e−03 | 7.75 | 1.95e−03 | 7.74 | 1.0960 |
| 128 | 1.11e−012 | 31.21 | 7.09e−013 | 31.21 | 7.88e−013 | 31.21 | 3.5520 |
| Theoretical order: 5 | | | | | | | |
| 16 | 7.25e−01 | 0.28 | 4.73e−01 | 0.40 | 5.22e−01 | 0.37 | 0.5920 |
| 32 | 2.59e−02 | 4.81 | 1.66e−02 | 4.84 | 1.84e−02 | 4.83 | 2.0200 |
| 64 | 8.90e−016 | 44.72 | 5.67e−016 | 44.73 | 6.30e−016 | 44.73 | 6.5200 |
| 128 | 6.04e−105 | 296.21 | 3.85e−105 | 296.21 | 4.27e−105 | 296.21 | 22.77 |

**Table 8**
Linear advection–reaction with HEOC-CITA. Output time $t_{out} = 1$ with $C_{cfl} = 0.9$, $\lambda = 1$ and $\beta = -10\,000$. Periodic boundary conditions are applied.

| Mesh | $L_\infty$-err | $L_\infty$-ord | $L_1$-err | $L_1$-ord | $L_2$-err | $L_2$-ord | CPU |
|---|---|---|---|---|---|---|---|
| Theoretical order: 2 | | | | | | | |
| 16 | 8.65e−01 | 0.05 | 5.63e−01 | 0.17 | 6.21e−01 | 0.14 | 0.0160 |
| 32 | 5.92e−01 | 0.55 | 3.78e−01 | 0.57 | 4.19e−01 | 0.57 | 0.0440 |
| 64 | 1.03e−01 | 2.52 | 6.53e−02 | 2.53 | 7.26e−02 | 2.53 | 0.1200 |
| 128 | 2.50e−04 | 8.69 | 1.52e−04 | 8.75 | 1.69e−04 | 8.75 | 0.4160 |
| Theoretical order: 3 | | | | | | | |
| 16 | 7.55e−01 | 0.20 | 4.93e−01 | 0.31 | 5.44e−01 | 0.28 | 0.0120 |
| 32 | 3.49e−01 | 1.11 | 2.23e−01 | 1.14 | 2.48e−01 | 1.13 | 0.0440 |
| 64 | 1.06e−02 | 5.04 | 6.75e−03 | 5.05 | 7.50e−03 | 5.05 | 0.1560 |
| 128 | 5.84e−08 | 17.47 | 3.72e−08 | 17.47 | 4.13e−08 | 17.47 | 0.6040 |
| Theoretical order: 4 | | | | | | | |
| 16 | 9.11e−01 | −0.03 | 5.95e−01 | 0.08 | 6.57e−01 | 0.06 | 0.1040 |
| 32 | 5.89e−01 | 0.63 | 3.77e−01 | 0.66 | 4.18e−01 | 0.65 | 0.3760 |
| 64 | 2.76e−03 | 7.74 | 1.76e−03 | 7.74 | 1.95e−03 | 7.74 | 1.6080 |
| 128 | 1.11e−012 | 31.21 | 7.09e−013 | 31.21 | 7.88e−013 | 31.21 | 4.6960 |
| Theoretical order: 5 | | | | | | | |
| 16 | 7.24e−01 | 0.28 | 4.73e−01 | 0.40 | 5.22e−01 | 0.37 | 1.1240 |
| 32 | 2.59e−02 | 4.81 | 1.66e−02 | 4.84 | 1.84e−02 | 4.83 | 3.8120 |
| 64 | 8.90e−016 | 44.72 | 5.66e−016 | 44.73 | 6.29e−016 | 44.73 | 14.972 |
| 128 | 6.04e−105 | 296.21 | 3.84e−105 | 296.21 | 4.27e−105 | 296.21 | 41.5960 |

$$\partial_t \mathbf{Q} + \partial_x \mathbf{F}(\mathbf{Q}) = \mathbf{S}(\mathbf{Q}) \,, \tag{56}$$

where $\mathbf{F}(\mathbf{Q})$ and $\mathbf{S}(\mathbf{Q})$ are given by (43). The Jacobian matrix $\mathbf{A}(\mathbf{Q})$ is given by

$$\mathbf{A} = \frac{1}{9}\begin{bmatrix} 5u - v & 2v - u \\ 4v - 2u & 4u + v \end{bmatrix} , \tag{57}$$

which can be decomposed as $\mathbf{A} = \mathbf{R}\mathbf{\Lambda}\mathbf{R}^{-1}$, with

$$\mathbf{R} = \begin{bmatrix} 1 & 1 \\ 2 & -1 \end{bmatrix} , \quad \mathbf{\Lambda} = \frac{1}{3}\begin{bmatrix} u + v & 0 \\ 0 & 2u - v \end{bmatrix} . \tag{58}$$

On the other hand, if we consider $\mathbf{W} = [w_1, w_2]^T$ defined as $\mathbf{W} = \mathbf{R}^{-1}\mathbf{Q}$, we obtain

$$w_1 = \frac{u + v}{3} \,, \; w_2 = \frac{2u - v}{3} \,. \tag{59}$$

After some manipulations, system (56) is transformed into

**Table 9**
Empirical convergence rates for ADER MT-HEOC-RITA applied to the non-linear system (56) with stiff source terms. Parameters are: $\beta = -1$, output time $t_{out} = 0.1$ and $C_{cfl} = 0.9$.

| Mesh | $L_\infty$-err | $L_\infty$-ord | $L_1$-err | $L_1$-ord | $L_2$-err | $L_2$-ord |
|---|---|---|---|---|---|---|
| Theoretical order: 2 | | | | | | |
| 64 | 1.11e−02 | 1.33 | 2.24e−03 | 2.20 | 3.17e−03 | 2.06 |
| 128 | 3.72e−03 | 1.57 | 4.76e−04 | 2.24 | 7.53e−04 | 2.07 |
| 256 | 1.36e−03 | 1.46 | 9.50e−05 | 2.32 | 1.84e−04 | 2.03 |
| 512 | 4.70e−04 | 1.53 | 2.03e−05 | 2.23 | 4.70e−05 | 1.97 |
| Theoretical order: 3 | | | | | | |
| 64 | 1.66e−03 | 2.07 | 2.32e−04 | 2.56 | 5.28e−04 | 2.32 |
| 128 | 2.75e−04 | 2.59 | 3.44e−05 | 2.75 | 8.15e−05 | 2.70 |
| 256 | 3.99e−05 | 2.78 | 4.69e−06 | 2.88 | 1.14e−05 | 2.83 |
| 512 | 5.37e−06 | 2.89 | 6.09e−07 | 2.94 | 1.50e−06 | 2.93 |
| Theoretical order: 4 | | | | | | |
| 64 | 1.27e−03 | 2.54 | 1.55e−04 | 3.10 | 3.52e−04 | 2.84 |
| 128 | 1.11e−04 | 3.52 | 1.12e−05 | 3.79 | 2.67e−05 | 3.72 |
| 256 | 6.52e−06 | 4.08 | 5.78e−07 | 4.28 | 1.44e−06 | 4.21 |
| 512 | 3.27e−07 | 4.32 | 2.88e−08 | 4.33 | 6.95e−08 | 4.37 |
| Theoretical order: 5 | | | | | | |
| 64 | 3.02e−03 | 1.14 | 1.91e−04 | 0.22 | 5.91e−04 | 0.35 |
| 128 | 1.23e−05 | 7.94 | 1.08e−06 | 7.47 | 2.86e−06 | 7.69 |
| 256 | 5.38e−07 | 4.52 | 4.33e−08 | 4.64 | 1.21e−07 | 4.57 |
| 512 | 2.55e−08 | 4.40 | 2.17e−09 | 4.32 | 4.68e−09 | 4.69 |

$$\partial_t w_1 + w_1 \partial_x (w_1) = 0 \,,$$
$$\partial_t w_2 + w_2 \partial_x (w_2) = \beta w_2^2 \,, \tag{60}$$

which is a decoupled system. The exact solutions of both equations are well known, they can be obtained by following the strategy in Appendix A. So, the exact solution to (56) is recovered as $\mathbf{RW} = \mathbf{Q}$, which in terms of $u$ and $v$ is given by

$$u(x,t) = w_1(x,t) + w_2(x,t) \,,$$
$$v(x,t) = 2w_1(x,t) - w_2(x,t) \,. \tag{61}$$

Results on the convergence rates study are shown in Tables 9 and 10 for ADER MT-HEOC-RITA and ADER MT-HEOC-CITA schemes, respectively. Tables 11 and 12 show the corresponding results for ADER MT-TT-RITA and ADER MT-TT-CITA schemes, respectively. We observe that in all four approaches the expected convergence rates are attained. Additionally, we observe from the tabulated errors that all approaches produce results with similar accuracy. These results suggest that for this test the variation CITA does not significantly improve the accuracy with respect to RITA.

CPU time comparisons are displayed in Table 13 for the four approaches. For second order of accuracy all schemes are similar, while for orders greater than three one begins to see a marked cost difference amongst the various schemes. The most striking difference occurs between HEOC (Harten and collaborators [23]) and TT (Toro and Titarev [43]). For the fifth order schemes the HEOC is about three times more expensive than the TT approach. Then there is also a difference in the way the derivatives are treated, with the RITA (reduced) being more efficient than CITA (complete). From these results and those of the convergence rates study it seems as if the scheme to be recommended for use is the TT scheme with the reduced treatment for derivatives (TT-RITA).

### 5.3. The LeVeque and Yee test

Here we apply our schemes to the well-known and challenging scalar test problem proposed by LeVeque and Yee [28], with a stiff non-linear source term. The flux function is $f(q) = \lambda q$ and the source term is $s(q) = \beta q(q-1)(q-\frac{1}{2})$, with $\lambda$ a constant speed of propagation and $\beta \leq 0$ a constant. For a general initial condition $q(x,0) = h(x)$ the exact solution can be found from the following algebraic equation for $q$

$$\frac{q(q-1)}{(q-1/2)^2} = \left( \frac{h(x-\lambda t))(h(x-\lambda t)-1)}{(h(x-\lambda t)-1/2)^2} \right) e^{\frac{\beta}{2} t} \,. \tag{62}$$

If we analyse the source term, we observe that critical points are $q = 0$, $q = 1/2$ and $q = 1$. That means, $s(0) = s(1/2) = s(1) = 0$. On the other hand, $s'(0) < 0$ and $s'(1) < 0$, whereas $s'(1/2) > 0$. Hence $q = 0$ and $q = 1$ are stable equilibrium points, so, $q(x(t), t)$ converges to one of theses values as $t$ increases. On the other hand, $q = 1/2$ is an unstable equilibrium point, so the solution away from it. Furthermore, for large values of $|\beta t|$, independently from the initial condition, the right-hand side goes to zero and thus the solution of $q(x,t)$ is forced to take the values $q(x,t) \equiv 0$ or $q(x,t) \equiv 1$. Therefore, this test transforms a smooth solution into a discontinuous one, which only takes values 0 and 1. For instance, let us consider the smooth initial condition

**Table 10**
Empirical convergence rates for ADER MT-HEOC-CITA applied to the non-linear system (56) with stiff source terms. Parameters are: $\beta = -1$, output time $t_{out} = 0.1$ and $C_{cfl} = 0.9$.

| Mesh | $L_\infty$-err | $L_\infty$-ord | $L_1$-err | $L_1$-ord | $L_2$-err | $L_2$-ord |
|---|---|---|---|---|---|---|
| Theoretical order: 2 | | | | | | |
| 64 | 1.27e−02 | 1.34 | 2.45e−03 | 2.10 | 3.46e−03 | 1.90 |
| 128 | 4.17e−03 | 1.61 | 6.04e−04 | 2.02 | 9.16e−04 | 1.92 |
| 256 | 1.47e−03 | 1.50 | 1.31e−04 | 2.20 | 2.25e−04 | 2.02 |
| 512 | 4.99e−04 | 1.56 | 2.68e−05 | 2.29 | 5.41e−05 | 2.06 |
| Theoretical order: 3 | | | | | | |
| 64 | 1.68e−03 | 1.72 | 2.41e−04 | 2.36 | 4.78e−04 | 2.00 |
| 128 | 2.93e−04 | 2.52 | 3.77e−05 | 2.67 | 7.99e−05 | 2.58 |
| 256 | 4.38e−05 | 2.74 | 5.22e−06 | 2.85 | 1.15e−05 | 2.80 |
| 512 | 5.85e−06 | 2.90 | 6.84e−07 | 2.93 | 1.52e−06 | 2.92 |
| Theoretical order : 4 | | | | | | |
| 64 | 1.31e−03 | 2.53 | 1.68e−04 | 3.14 | 3.64e−04 | 2.87 |
| 128 | 1.12e−04 | 3.56 | 1.19e−05 | 3.82 | 2.70e−05 | 3.75 |
| 256 | 6.49e−06 | 4.10 | 6.13e−07 | 4.28 | 1.44e−06 | 4.23 |
| 512 | 3.24e−07 | 4.32 | 3.03e−08 | 4.34 | 6.91e−08 | 4.38 |
| Theoretical order: 5 | | | | | | |
| 64 | 2.92e−04 | 4.38 | 3.12e−05 | 5.00 | 7.28e−05 | 4.70 |
| 128 | 1.24e−05 | 4.56 | 1.28e−06 | 4.61 | 3.13e−06 | 4.54 |
| 256 | 5.39e−07 | 4.52 | 4.25e−08 | 4.92 | 1.20e−07 | 4.71 |
| 512 | 2.55e−08 | 4.40 | 2.15e−09 | 4.30 | 4.66e−09 | 4.68 |

**Table 11**
Empirical convergence rates for ADER MT-TT-RITA applied to the non-linear system (56) with stiff source terms. Parameters are: $\beta = -1$, output time $t_{out} = 0.1$ and $C_{cfl} = 0.9$.

| Mesh | $L_\infty$-err | $L_\infty$-ord | $L_1$-err | $L_1$-ord | $L_2$-err | $L_2$-ord |
|---|---|---|---|---|---|---|
| Theoretical order: 2 | | | | | | |
| 64 | 1.11e−02 | 1.33 | 2.24e−03 | 2.20 | 3.17e−03 | 2.06 |
| 128 | 3.72e−03 | 1.57 | 4.76e−04 | 2.24 | 7.53e−04 | 2.07 |
| 256 | 1.36e−03 | 1.46 | 9.50e−05 | 2.32 | 1.84e−04 | 2.03 |
| 512 | 4.70e−04 | 1.53 | 2.03e−05 | 2.23 | 4.70e−05 | 1.97 |
| Theoretical order: 3 | | | | | | |
| 64 | 1.66e−03 | 2.07 | 2.32e−04 | 2.56 | 5.28e−04 | 2.32 |
| 128 | 2.75e−04 | 2.59 | 3.44e−05 | 2.75 | 8.15e−05 | 2.70 |
| 256 | 3.99e−05 | 2.78 | 4.69e−06 | 2.88 | 1.14e−05 | 2.83 |
| 512 | 5.37e−06 | 2.89 | 6.09e−07 | 2.94 | 1.50e−06 | 2.93 |
| Theoretical order: 4 | | | | | | |
| 64 | 1.27e−03 | 2.54 | 1.55e−04 | 3.10 | 3.52e−04 | 2.84 |
| 128 | 1.11e−04 | 3.52 | 1.12e−05 | 3.79 | 2.67e−05 | 3.72 |
| 256 | 6.52e−06 | 4.08 | 5.78e−07 | 4.28 | 1.44e−06 | 4.21 |
| 512 | 3.27e−07 | 4.32 | 2.88e−08 | 4.33 | 6.95e−08 | 4.37 |
| Theoretical order: 5 | | | | | | |
| 60 | 2.74e−03 | 0.12 | 1.63e−04 | 1.40 | 5.08e−04 | 0.85 |
| 120 | 2.46e−05 | 6.80 | 1.40e−06 | 6.86 | 4.26e−06 | 6.90 |
| 240 | 7.25e−07 | 5.09 | 5.89e−08 | 4.58 | 1.64e−07 | 4.70 |
| 480 | 3.33e−08 | 4.44 | 2.73e−09 | 4.43 | 6.06e−09 | 4.76 |

$$h(x) = 0.1 + .5\sin(2\pi x)^2\,, \tag{63}$$

and the computational domain $[0, 1]$ with periodic boundary conditions $\lambda = 1$, $\beta = -1000$, $t_{out} = 0.15$ and CFL number $c_{cfl} = 0.1$. Fig. 7 shows the exact solution (full line) and numerical solutions obtained with ADER MT-HEOC-RITA of third (square) and fifth (circles) orders of accuracy. In the figure we note that the smooth initial condition (star plus dotted line) evolves into a piecewise constant function, discontinuous function, as expected. Table 14 shows the result of the convergence rate assessment, we note that expected theoretical orders of accuracy are not achieved. Furthermore, the convergence rates decrease, which indicates that mesh refinement will have a low impact on the formal accuracy of solutions. Consequently, the order of accuracy cannot be assessed for this test. However, it is relevant to show that the same schemes shown to be of high-order of accuracy for smooth solutions for stiff problems can also compute very good approximations to stiff problems with shock waves, as illustrated in the following test.

Let us consider the computational domain $[0, 1]$, transmissive boundary conditions and the initial condition

**Table 12**
Empirical convergence rates for ADER MT-TT-CITA applied to the non-linear system (56) with stiff source terms. Parameters are: $\beta = -1$, output time $t_{out} = 0.1$ and $C_{cfl} = 0.9$.

| Mesh | $L_\infty$-err | $L_\infty$-ord | $L_1$-err | $L_1$-ord | $L_2$-err | $L_2$-ord |
|---|---|---|---|---|---|---|
| Theoretical order: 2 | | | | | | |
| 64 | 1.11e−02 | 1.33 | 2.24e−03 | 2.20 | 3.17e−03 | 2.06 |
| 128 | 3.72e−03 | 1.57 | 4.76e−04 | 2.24 | 7.53e−04 | 2.07 |
| 256 | 1.36e−03 | 1.46 | 9.50e−05 | 2.32 | 1.84e−04 | 2.03 |
| 512 | 4.70e−04 | 1.53 | 2.03e−05 | 2.23 | 4.70e−05 | 1.97 |
| Theoretical order: 3 | | | | | | |
| 64 | 1.66e−03 | 2.07 | 2.32e−04 | 2.56 | 5.28e−04 | 2.32 |
| 128 | 2.75e−04 | 2.59 | 3.44e−05 | 2.75 | 8.15e−05 | 2.70 |
| 256 | 3.99e−05 | 2.78 | 4.69e−06 | 2.88 | 1.14e−05 | 2.83 |
| 512 | 5.37e−06 | 2.89 | 6.09e−07 | 2.94 | 1.50e−06 | 2.93 |
| Theoretical order: 4 | | | | | | |
| 64 | 1.27e−03 | 2.54 | 1.55e−04 | 3.10 | 3.52e−04 | 2.84 |
| 128 | 1.11e−04 | 3.52 | 1.12e−05 | 3.79 | 2.67e−05 | 3.72 |
| 256 | 6.52e−06 | 4.08 | 5.78e−07 | 4.28 | 1.44e−06 | 4.21 |
| 512 | 3.27e−07 | 4.32 | 2.88e−08 | 4.33 | 6.95e−08 | 4.37 |
| Theoretical order: 5 | | | | | | |
| 60 | 2.74e−03 | 0.12 | 1.63e−04 | 1.40 | 5.08e−04 | 0.85 |
| 120 | 2.46e−05 | 6.80 | 1.40e−06 | 6.86 | 4.26e−06 | 6.90 |
| 240 | 7.25e−07 | 5.09 | 5.89e−08 | 4.58 | 1.64e−07 | 4.70 |
| 480 | 3.33e−08 | 4.44 | 2.73e−09 | 4.43 | 6.06e−09 | 4.76 |

**Table 13**
CPU time comparisons for solvers HEOC-RITA, HEOC-CITA, TT-RITA and TT-CITA as applied to the non-linear system (56) with stiff source terms, with parameters $\beta = -1$, output time $t_{out} = 0.1$ and $C_{cfl} = 0.9$.

| Mesh | HEOC-RITA | HEOC-CITA | TT-RITA | TT-CITA |
|---|---|---|---|---|
| CPU for order: 2 | | | | |
| 64 | 0.158 | 0.200 | 0.150 | 0.064 |
| 128 | 0.535 | 0.817 | 0.482 | 0.215 |
| 256 | 2.161 | 2.814 | 1.453 | 0.872 |
| 512 | 7.856 | 12.199 | 5.403 | 3.296 |
| CPU for order: 3 | | | | |
| 64 | 0.475 | 2.321 | 0.680 | 1.065 |
| 128 | 1.666 | 6.326 | 2.419 | 3.533 |
| 256 | 10.630 | 19.144 | 9.063 | 8.551 |
| 512 | 38.237 | 106.231 | 33.933 | 44.948 |
| CPU for order: 4 | | | | |
| 64 | 5.548 | 59.510 | 4.876 | 13.774 |
| 128 | 11.634 | 167.250 | 15.928 | 99.181 |
| 256 | 68.693 | 530.989 | 36.104 | 189.584 |
| 512 | 215.524 | 2611.530 | 126.663 | 746.642 |
| CPU for order: 5 | | | | |
| 64 | 52.938 | 715.561 | 35.220 | 281.695 |
| 128 | 183.363 | 2908.111 | 123.132 | 1042.716 |
| 256 | 678.655 | 11 685.232 | 453.159 | 3949.903 |
| 512 | 1551.380 | 42 010.201 | 1187.801 | 15 182.973 |

$$q(x,0) = \begin{cases} 1 & \text{if } x < 0.3\,, \\ 0 & \text{if } x > 0.3\,. \end{cases} \tag{64}$$

Fig. 8 shows a comparison between exact (line) and numerical (symbols) solutions of third and fifth orders of accuracy, obtained with ADER in conjunction with the RITA applied to the TT and HEOC frameworks for solving the GRP. Parameters are: $\lambda = 1$, $t_{out} = 0.3$, for $\beta = -1000$, $N = 150$ cells and $C_{cfl} = 0.3$. All numerical solutions are correct, there are no spurious oscillations and the discontinuity travels with the correct speed. The increased formal accuracy increases the resolution of the shock (narrower).

## 6. Conclusions

We have presented a new, implicit, approach to calculate the semi-analytical solution to the generalized Riemann problem for non-linear hyperbolic systems with stiff source terms. To start with, we propose an implicit version of the Taylor

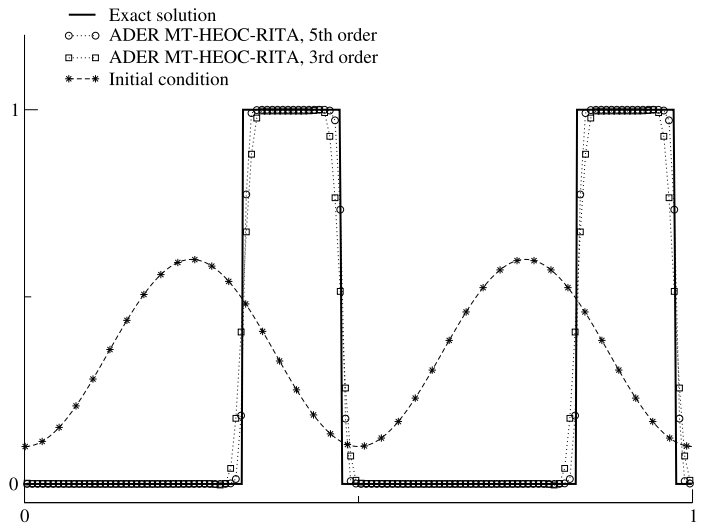


**Fig. 7.** ADER MT-HEOC-RITA scheme. LeVeque and Yee test with continuous initial condition $h(x) = 0.1 + .5\sin(2\pi x)^2$ (star plus dotted line). Comparison of exact solution (full line) with third order (squared symbols) ADER solution and the fifth order (circles) ADER solution. Parameters: $\lambda = 1$, $\beta = -1000$, output time $t_{out} = 0.15$, 128 cells and $C_{cfl} = 0.1$.

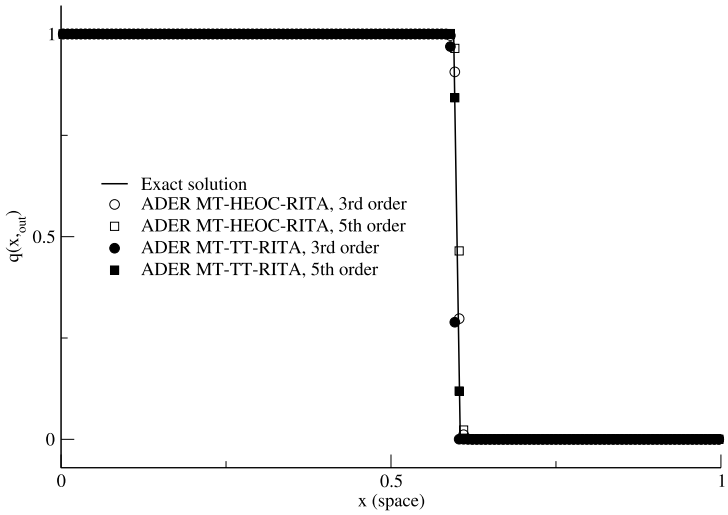


**Fig. 8.** LeVeque and Yee test. Comparison between the exact solution (full line) and ADER numerical solutions of third and fifth orders of accuracy. Computational parameters are: $\lambda = 1$, $t_{out} = 0.3$, for $\beta = -1000$, $N = 150$ cells and $C_{cfl} = 0.3$.

series expansion suggested by Le Floch and Raviart [27] and used by Toro and Titarev [43] to produce their explicit GRP solver (the TT solver). Then, the present solver makes use of the Cauchy–Kowalewskaya procedure in the implicit Taylor series expansion. The implicit methodology extends both the TT approach [43] and the HEOC approach [23,8]. In addition, the methodology requires a careful treatment of spatial derivatives. We have investigated two approaches to evolve these spatial derivatives, namely (i) full implicit Taylor series expansion considering $M$ terms (CITA) and (ii) reduced implicit Taylor series expansion approach (RITA), where the evolution in time of the $l$-th spatial derivatives is approximated with an implicit Taylor expansion containing $M - l$ terms. The complete GRP solution results from a non-linear algebraic system, for which fixed-point iteration procedures play a key role. Here we have used the standard Newton reduced-step method and we have simply taken the reconstruction polynomials as the starting guess. The new GRP solver has been analysed for a model linear equation and has been assessed comprehensively for a suit of test problems involving stiff source terms. Four combinations of schemes have been proposed, with the TT and HEOC frameworks implemented with RITA and CITA variations to treat the space derivatives.

All schemes for solving the GRP have then been implemented in the numerical ADER approach for solving the general IBVP to high order of accuracy. The resulting ADER schemes remain globally explicit, with a locally implicit solver for the GRP. Convergence rates studies show that the resulting ADER schemes reconcile stiffness with high order of accuracy in space and time. Schemes of up to 5th order of accuracy were implemented, but the approach permits arbitrary orders of

**Table 14**
Empirical convergence rates for ADER MT-HEOC-RITA applied to the LeVeque and Yee with a continuous initial condition. Parameters are: $\lambda = 1$, $\beta = -1000$, output time $t_{out} = 0.15$ and $C_{cfl} = 0.1$.

| Mesh | $L_\infty$-err | $L_\infty$-ord | $L_1$-err | $L_1$-ord | $L_2$-err | $L_2$-ord |
|---|---|---|---|---|---|---|
| Theoretical order: 2 | | | | | | |
| 64 | 3.33e−01 | −0.35 | 2.77e−02 | 0.74 | 8.68e−02 | 0.22 |
| 128 | 9.24e−01 | −1.47 | 4.68e−02 | −0.76 | 1.83e−01 | −1.07 |
| 256 | 9.99e−01 | −0.11 | 5.15e−02 | −0.14 | 2.09e−01 | −0.19 |
| 512 | 10.00e−01 | −0.00 | 4.93e−02 | 0.06 | 2.12e−01 | −0.02 |
| Theoretical order: 3 | | | | | | |
| 64 | 2.20e−01 | 0.79 | 2.19e−02 | 1.08 | 5.82e−02 | 0.86 |
| 128 | 2.22e−01 | −0.02 | 9.64e−03 | 1.19 | 3.64e−02 | 0.67 |
| 256 | 2.22e−01 | 0.00 | 7.20e−03 | 0.42 | 3.24e−02 | 0.17 |
| 512 | 3.72e−01 | −0.75 | 5.43e−03 | 0.41 | 3.40e−02 | −0.07 |
| Theoretical order: 4 | | | | | | |
| 64 | 9.34e−01 | 0.10 | 1.23e−01 | 1.43 | 3.00e−01 | 0.83 |
| 128 | 9.35e−01 | −0.00 | 7.06e−02 | 0.81 | 2.31e−01 | 0.38 |
| 256 | 9.84e−01 | −0.07 | 4.69e−02 | 0.59 | 1.90e−01 | 0.28 |
| 512 | 1.00e−00 | −0.03 | 2.73e−02 | 0.78 | 1.45e−01 | 0.39 |
| Theoretical order: 5 | | | | | | |
| 64 | 2.45e−01 | 1.95 | 2.05e−02 | 3.00 | 5.82e−02 | 2.46 |
| 128 | 2.26e−01 | 0.11 | 9.62e−03 | 1.09 | 3.95e−02 | 0.56 |
| 256 | 2.79e−01 | −0.30 | 6.24e−03 | 0.62 | 3.56e−02 | 0.15 |
| 512 | 1.00e−00 | −0.03 | 2.73e−02 | 0.78 | 1.45e−01 | 0.39 |

accuracy in both space and time. CPU time comparisons for the four approaches reveal that for second order of accuracy all schemes are similar, while for orders greater than three one sees a marked cost difference amongst the various schemes. The most striking difference occurs between HEOC (Harten and collaborators [23]) and TT (Toro and Titarev [43]). For the fifth order schemes the HEOC is about three times more expensive than the TT approach. Then there is also a difference in the way the derivatives are treated, with the RITA (reduced) being more efficient than CITA (complete). From these results and those of the convergence rates study it seems as if the scheme to be recommended for use is the TT scheme with the reduced treatment for derivatives (TT-RITA).

## Appendix A. On a strategy to compute analytical solutions to the Burgers equations with special source terms and continuous initial conditions

In this appendix we present the Burgers equation with source terms and describe some characteristics to be satisfied for the source terms in order to obtain exact solutions. To start with, let us consider a balance law in the form

$$\left.\begin{aligned} \partial_t q(x,t) + \partial_x\left(\tfrac{q(x,t)^2}{2}\right) = s(q(x,t))\,, \\ q(x,0) = h_0(x)\,, \end{aligned}\right\} \tag{A.1}$$

where $h_0(x)$ is a regular initial condition and $s(q)$ is the source term. To solve this type of balance laws we use the characteristic method. Hence, we take $x$ in the $x$–$t$ plane to be the curve satisfying

$$\left.\begin{aligned} \tfrac{d}{dt}x(t) = q(x(t),t)\,, \\ x(0) = y\,, \end{aligned}\right\} \tag{A.2}$$

with $y$ a constant value. We denote this ODE as *characteristic ODE*. On the other hand, we can define

$$\hat{q}(t) := q(x(t),t)\,,\quad h(0) := q(x(0),0) = h_0(y)\,, \tag{A.3}$$

where $y$ is that given in (A.2). Then, through the characteristic curve $x(t)$, the balance law (A.1) becomes an ODE given by

$$\left.\begin{aligned} \tfrac{d}{dt}\hat{q}(t) = s(\hat{q}(t))\,, \\ \hat{q}(0) = h(0)\,. \end{aligned}\right\} \tag{A.4}$$

This ODE is called here *equivalent ODE*. The next lemma ensures the existence of solutions for the *equivalent ODE*.

**Lemma A.1.** *If $s(\hat{q})^{-1}$ contains a primitive function, then the equivalent ODE is solvable. Additionally, there exists a function $\mathcal{E}(t, h(0))$ such that*

$$\left.\begin{array}{l} \frac{\partial}{\partial t}\mathcal{E}(t,h(0)) = s(\hat{q}(t)) \,, \\ \mathcal{E}(0,h(0)) = h(0) \end{array}\right\} \tag{A.5}$$

*and* $\hat{q}(t) = \mathcal{E}(t,h(0))$.

**Proof.** We integrate (A.4) as follows

$$\int_{h(0)}^{\hat{q}(t)} s(q)^{-1} dq = \int_0^t dt \,, \tag{A.6}$$

as $s(q)^{-1}$ has a primitive, there exists a function $G(q)$ such that

$$\frac{d}{dq} G(q) = s(q)^{-1} \,. \tag{A.7}$$

Therefore, $\mathcal{E}(t,h(0))$ is the solution to $G(\mathcal{E}) - G(h(0)) - t = 0$. So, if there exists the inverse function of $G(q)$, which is denoted here by $G^{-1}(q)$, the function $\mathcal{E}$ is explicitly given by

$$\mathcal{E}(t,h(0)) = G^{-1}(t + G(h(0))) \,. \tag{A.8}$$

In any case the exact solution is obtained as

$$\hat{q}(t) = \mathcal{E}(t,h(0)) \,. \qquad \square \tag{A.9}$$

Once the solution to the *equivalent ODE* is available and observing that $h(0) := h_0(y)$, the *characteristic ODE* takes the form

$$\left.\begin{array}{l} \frac{d}{dt} x(t) = \mathcal{E}(t,h_0(y)) \,, \\ x(0) = y \,. \end{array}\right\} \tag{A.10}$$

The existence of solutions of this ODE is given in the following.

**Lemma A.2.** *If* $\mathcal{E}(t,h_0(y)$ *has a primitive function* $\mathcal{F}(t,h_0(y))$ *with respect to* $t$, *such that* $\frac{d}{dt}\mathcal{F}(t,h_0(y)) = \mathcal{E}(t,h_0(y))$ *and* $\mathcal{F}(0,h_0(y)) = 0$, *then, the characteristic ODE has the exact solution*

$$x = y + \mathcal{F}(t,h_0(y)) \,. \tag{A.11}$$

**Proof.** Integrating the ODE (A.10), we obtain

$$\int_y^x dx = \int_0^t \mathcal{E}(t,h_0(y))dt \,. \tag{A.12}$$

So, by using the properties of $\mathcal{F}(t,h_0(y))$, the result follows. $\square$

**Remark 2.** The value $y$ is a constant for the characteristic ODE (A.10). However, if values $x$ and $t$ are set in (A.11), there exists a constant $y$ satisfying (A.11). Therefore we can identify such constant by $y = y(x,t)$.

**Proposition A.3.** *If* $s(q)^{-1}$ *and* $\mathcal{E}(t,h_0(y))$ *have their respective primitive functions, then the problem (A.1) has the exact solution*

$$q(x,t) = \mathcal{E}(t,h_0(y)) \,, \tag{A.13}$$

*where* $y$ *satisfies*

$$x = y + \mathcal{F}(t,h_0(y)) \,, \tag{A.14}$$

*with* $\mathcal{F}(t,h_0(y))$ *the primitive of* $\mathcal{E}(t,h_0(y))$ *with respect of* $t$.

**Proof.** The construction of this function is given by Lemmas A.1 and A.2. Now, we are going to prove that $q(x,t)$ solves (A.1). Note that by the chain rule

$$\left.\begin{array}{rl} \partial_t q = & \frac{\partial}{\partial y}\mathcal{E}\frac{\partial y}{\partial t} + \frac{\partial}{\partial t}\mathcal{E} \,, \\ \partial_x q = & \frac{\partial}{\partial y}\mathcal{E}\frac{\partial y}{\partial x} \,. \end{array}\right\} \tag{A.15}$$

Then

$$\partial_t q + q\partial_x q = \frac{\partial}{\partial y}\mathcal{E}(\frac{\partial y}{\partial t} + q\frac{\partial y}{\partial x}) + \frac{\partial}{\partial t}\mathcal{E}\,. \tag{A.16}$$

On the other hand we have

$$\begin{aligned} 0 &= \frac{\partial y}{\partial t} + \frac{\partial}{\partial t}\mathcal{F} + \frac{\partial}{\partial(h_0)}\mathcal{F}h_0(y)'\frac{\partial y}{\partial t}\,, \\ 1 &= \frac{\partial y}{\partial x} + \frac{\partial}{\partial(h_0)}\mathcal{F}h_0(y)'\frac{\partial y}{\partial x}\,. \end{aligned} \tag{A.17}$$

Therefore, as $\mathcal{F}$ is the primitive of $\mathcal{E}$, we have

$$\frac{\partial y}{\partial t} + q\frac{\partial y}{\partial x} = \left(1 + \frac{\partial}{\partial h_0}Fh_0'\right)^{-1}(-\frac{\partial}{\partial t}\mathcal{F} + q) = 0\,. \tag{A.18}$$

Finally, we note that

$$\frac{\partial}{\partial t}\mathcal{E}(t, h_0(y)) = s(q(x,t)) \tag{A.19}$$

and so the result holds. □

Applying this methodology we solve the Burgers equation with a quadratic source term.

### A.1. Burgers' equation with a quadratic source term

Let us consider the partial differential equation

$$\left.\begin{aligned} \partial_t q(x,t) + \partial_x\left(\frac{q(x,t)^2}{2}\right) &= \beta q(x,t)^2\,, \\ q(x,t) &= h_0(x)\,. \end{aligned}\right\} \tag{A.20}$$

The *equivalent ODE* has the form

$$\left.\begin{aligned} \frac{d\hat{q}(t)}{dt} &= \beta\hat{q}(t)^2\,, \\ \hat{q}(0) &= h(0)\,, \end{aligned}\right\} \tag{A.21}$$

which is solvable and the exact solution is

$$\hat{q}(t) = \mathcal{E}(t, h(0)) = \frac{h(0)}{1 - \beta t h(0)}\,. \tag{A.22}$$

On the other hand we note that the *characteristic ODE*

$$\left.\begin{aligned} \frac{d}{dt}x(t) &= q(x,t)\,, \\ x(0) &= y\,, \end{aligned}\right\} \tag{A.23}$$

for $q(x,t)$ satisfying (A.22) has the solution

$$x = y - \frac{ln(1 - \beta t h_0(y))}{\beta}\,. \tag{A.24}$$

Therefore, the solution of (A.20) is given by

$$q(x,t) = \frac{h_0(y)}{1 - \beta t h_0(y)}\,, \tag{A.25}$$

with $y$ a solution of (A.24).

**Example 1.** Let us consider (A.20) in the interval $[0,1]$, with initial condition

$$h_0(x) = \sin(2\pi x)\,. \tag{A.26}$$

With this choice $y$ is not explicitly obtained from (A.24). Therefore we use the bisection method. Fig. 9, shows the initial condition (dashed line) and the solution (full line) at $t_{out} = 0.15$ and for $\beta = -2$.

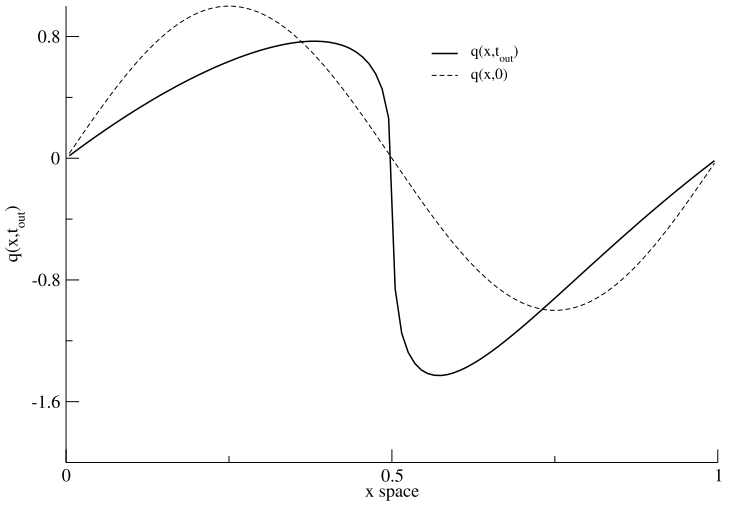


**Fig. 9.** Burgers equation with quadratic source term. Initial condition (dashed line) and the exact solution (full line) at time $t_{out} = 0.15$, for $\beta = -2$.

## Appendix B. On fixed point iteration procedures and their assessment for solving algebraic systems

In this appendix we illustrate how to implement two fixed-point procedures and compare their performance. Here the conventional Newton and the Newton reduced-step methods are considered for solving problems of the form

$$\mathbf{H}(\mathbf{U}) = \mathbf{0}\,, \tag{B.1}$$

where (B.1) is a system of algebraic equations with $\mathbf{H}(\mathbf{U}), \mathbf{U} \in \mathbb{R}^m$.

It is well known that conventional Newton method solves (B.1) through the following sequence

$$\mathbf{U}^{k+1} = \mathbf{U}^k - \delta^k\,, \tag{B.2}$$

where $\delta^k$ is the solution of

$$\mathbf{J}_H(\mathbf{U}^k)\delta^k = \mathbf{H}(\mathbf{U}^k)\,, \tag{B.3}$$

with $\mathbf{J_H}(\mathbf{U})$ the Jacobian matrix of $\mathbf{H}(\mathbf{U})$ with respect to $\mathbf{U}$. On the other hand, the Newton reduced-step method is given by

$$\mathbf{U}^{k+1} = \mathbf{U}^k - \delta_i^k\,, \tag{B.4}$$

where

$$\delta_{i+1}^k = \begin{cases} \delta_i^k \text{ and stop}, & \text{if } ||\delta_i^k|| < \eta\,, \\ \mu\delta_i^k, & \text{if } ||\delta_i^k|| \geq \eta\,, \end{cases} \tag{B.5}$$

with $\mu = 0.5$, $\eta = 10^{-2}$, $0 \leq i \leq 3$ where $\delta_0^k$ is the solution of

$$\mathbf{J}_H(\mathbf{U}^k)\delta_0^k = \mathbf{H}(\mathbf{U}^k)\,. \tag{B.6}$$

Newton reduce-step carries out less evaluations of Jacobian matrix and solutions of linear systems than conventional Newton method. Both procedures start from the initial guess $\mathbf{U}^0$, which is obtained from the reconstruction polynomials and its derivatives. Additionally, both methods stop when the following criterion is satisfied

$$||\delta^k|| < \epsilon := 10^{-6}\,. \tag{B.7}$$

### *B.1. How to quantify the number of iterations for fixed point procedures*

To quantify the number of iterations associated to a single time step of the ADER schemes, we are going to measure the number of fixed point iterations involved in the source evaluation. In each cell $i$ the implicit GRP solver is called $n_{GP}^2$ times; so, the arithmetic mean in the cell $i$ can be obtained. It will be denoted by $FPI_i$. Therefore, we can now compute the global mean iteration $\bar{A}_{FPI}^n$ in a step $n$ of the ADER scheme. This is done by taking the mean values of all the $FPI_i$

$$\bar{A}_{FPI}^n = \sum_{i=1}^{N} \frac{FPI_i}{N}\,. \tag{B.8}$$

Similarly, a standard deviation can be computed as follows

**Table 15**
Linear advection–reaction equation. Conventional Newton and Newton reduced-step methods. $A_{CN}$: mean iterations for the conventional Newton method, $\sigma_{CN}$: standard deviation for the conventional Newton method, $A_{NRS}$: mean iterations for the Newton reduced-step method, $\sigma_{NRS}$: standard deviation for the Newton reduced-step method. Parameters $t_{out} = 1$, 128 cells, $C_{cfl} = 0.9$, $\lambda = 1$ and $\beta = -10$.

| Ord | $A_{CN} \pm \sigma_{CN}$ | $A_{NRS} \pm \sigma_{NRS}$ | $A_{CN} \pm \sigma_{CN}$ | $A_{NRS} \pm \sigma_{NRS}$ |
|---|---|---|---|---|
| | HEOC-RITA | | HEOC-CITA | |
| 2 | $1 \pm 0$ | $1 \pm 0$ | $0.51 \pm 0.26$ | $0.51 \pm 0.26$ |
| 3 | $1 \pm 0$ | $1 \pm 0$ | $0.94 \pm 0.13$ | $0.94 \pm 0.13$ |
| 4 | $1 \pm 0$ | $1 \pm 0$ | $1 \pm 0$ | $1 \pm 0$ |
| 5 | $1 \pm 0$ | $1 \pm 0$ | $1 \pm 0$ | $1 \pm 0$ |
| | TT-RITA | | TT-CITA | |
| 2 | $1 \pm 0$ | $1 \pm 0$ | $1 \pm 0$ | $1 \pm 0$ |
| 3 | $1 \pm 0$ | $1 \pm 0$ | $1 \pm 0$ | $1 \pm 0$ |
| 4 | $1 \pm 0$ | $1 \pm 0$ | $1 \pm 0$ | $1 \pm 0$ |
| 5 | $1 \pm 0$ | $1 \pm 0$ | $1 \pm 0$ | $1 \pm 0$ |

**Table 16**
LeVeque and Yee test. Conventional Newton and Newton reduced-step methods. $A_{CN}$: mean iterations for the conventional Newton method, $\sigma_{CN}$: standard deviation for the conventional Newton method, $A_{NRS}$: mean iterations for the Newton reduced-step method, $\sigma_{NRS}$: standard deviation for the Newton reduced-step method. Parameters $t_{out} = 0.1$, 150 cells, $C_{cfl} = 0.1$ and $\beta = -1000$.

| Ord | $A_{CN} \pm \sigma_{CN}$ | $A_{NRS} \pm \sigma_{NRS}$ | $A_{CN} \pm \sigma_{CN}$ | $A_{NRS} \pm \sigma_{NRS}$ |
|---|---|---|---|---|
| | HEOC-RITA | | HEOC-CITA | |
| 2 | $1.39 \pm 0.23$ | $2.24 \pm 0.86$ | $1.09 \pm 0.37$ | $1.92 \pm 0.87$ |
| 3 | $1.81 \pm 0.35$ | $1.81 \pm 0.88$ | $1.14 \pm 0.46$ | $1.87 \pm 0.89$ |
| 4 | $1.13 \pm 0.44$ | $1.25 \pm 0.55$ | $1.22 \pm 0.60$ | $1.36 \pm 0.71$ |
| 5 | $1.18 \pm 0.57$ | $1.30 \pm 0.67$ | $1.13 \pm 0.52$ | $1.45 \pm 1.32$ |
| | TT-RITA | | TT-CITA | |
| 2 | $1.05 \pm 0.26$ | $1.88 \pm 0.87$ | $1.09 \pm 0.37$ | $1.96 \pm 0.87$ |
| 3 | $1.08 \pm 0.34$ | $1.82 \pm 0.89$ | $1.11 \pm 0.45$ | $1.93 \pm 0.91$ |
| 4 | $1.16 \pm 0.48$ | $1.28 \pm 0.58$ | $1.14 \pm 0.55$ | $1.39 \pm 0.65$ |
| 5 | $1.19 \pm 0.58$ | $1.30 \pm 0.68$ | $1.14 \pm 0.55$ | $1.39 \pm 0.65$ |

$$\sigma_{FPI}^{n} = \left( \sum_{i=1}^{N} \frac{(FPI_i - \bar{A}_{FPI})^2}{N} \right)^{\frac{1}{2}}, \tag{B.9}$$

here $N$ is assumed to be the number of cells. If an ADER scheme computes its solution in $N_{max}$ time steps, then global estimators can now be obtained from

$$\left.\begin{aligned} A_k &= \frac{1}{N_{max}} \sum_{n}^{N_{max}} \bar{A}_{FPI}^{n}, \\ \sigma_k &= \frac{1}{N_{max}} \sum_{n}^{N_{max}} \sigma_{FPI}^{n}, \end{aligned}\right\} \tag{B.10}$$

where $k$ takes values *CN* and *NRS*, which stand by Conventional Newton and Newton Reduce-Step, respectively. In the following section we apply these global estimators for numerical examples seen in this paper.

### *B.2. Assessment of tests*

In this section we compute the global estimator (B.10) in order to quantify the performance of fixed point iteration procedures. Here the estimators are computed for the linear advection–reaction equation, the LeVeque and Yee test and a non-linear system. Here ADER HEOC and the ADER TT schemes in their implicit versions will be applied.

Table 15 shows the mean iterations and standard deviations for the linear advection–reaction equation. In the table we depict the results for 128 cells, $C_{cfl} = 0.9$, $\lambda = 1$ and $\beta = -10$. Notice that for these parameters the expected orders of accuracy are achieved. We observe that number of iterations are those expected for the linear case.

Table 16 shows the estimators for the LeVeque and Yee test. We remark that orders of accuracy are not achieved for this test due to the lack of regularity of the solution. However, the parameters $t_{out} = 0.1$, 150 cells, $C_{cfl} = 0.1$ and $\beta = -1000$, are chosen in order to ensure that the numerical solution provides a correct description of the wave propagation. For a

**Table 17**
Non-linear system. Conventional Newton and Newton reduced-step methods. $A_{CN}$: mean iterations for the conventional Newton method, $\sigma_{CN}$: standard deviation for the conventional Newton method, $A_{NRS}$: mean iterations for the Newton reduced-step method, $\sigma_{NRS}$: standard deviation for the Newton reduced-step method. Parameters $t_{out} = 0.1$, 128 cells, $C_{cfl} = 0.9$ and $\beta = -1$.

| Ord | $A_{CN} \pm \sigma_{CN}$ | $A_{NRS} \pm \sigma_{NRS}$ | $A_{CN} \pm \sigma_{CN}$ | $A_{NRS} \pm \sigma_{NRS}$ |
|---|---|---|---|---|
| | HEOC-RITA | | HEOC-CITA | |
| 2 | $1.34 \pm 0.21$ | $2.39 \pm 0.20$ | $2.78 \pm 0.16$ | $2.77 \pm 0.20$ |
| 3 | $1.80 \pm 0.11$ | $2.80 \pm 0.09$ | $3.03 \pm 0.07$ | $3.20 \pm 0.36$ |
| 4 | $2.00 \pm 0.25$ | $2.00 \pm .25$ | $3.30 \pm 0.08$ | $3.33 \pm 0.33$ |
| 5 | $2.30 \pm 0.31$ | $2.30 \pm 0.31$ | $3.67 \pm 0.04$ | $3.68 \pm 0.50$ |
| | TT-RITA | | TT-CITA | |
| 2 | $2.21 \pm 0.19$ | $2.21 \pm 0.19$ | $2.78 \pm 0.16$ | $2.80 \pm 0.19$ |
| 3 | $2.79 \pm 0.08$ | $2.79 \pm 0.09$ | $3.03 \pm 0.07$ | $3.08 \pm 0.14$ |
| 4 | $2.93 \pm 0.12$ | $2.99 \pm 0.20$ | $3.30 \pm 0.19$ | $3.53 \pm 0.33$ |
| 5 | $3.30 \pm 0.20$ | $3.57 \pm 0.28$ | $3.67 \pm 0.08$ | $3.78 \pm 0.24$ |

**Table 18**
Non-linear system. Conventional Newton and Newton reduced-step methods. $A_{CN}$: mean iterations for the conventional Newton method, $\sigma_{CN}$: standard deviation for the conventional Newton method, $A_{NRS}$: mean iterations for the Newton reduced-step method, $\sigma_{NRS}$: standard deviation for the Newton reduced-step method. Parameters $\epsilon = 5 \cdot 10^{-14}$, $t_{out} = 0.1$, 128 cells, $C_{cfl} = 0.9$ and $\beta = -1$.

| Ord | $A_{CN} \pm \sigma_{CN}$ | $A_{NRS} \pm \sigma_{NRS}$ |
|---|---|---|
| | TT-RITA | |
| 2 | $3.05 \pm 0.11$ | $4.21 \pm 0.37$ |
| 3 | $2.80 \pm 0.09$ | $2.99 \pm 0.20$ |
| 4 | $3.81 \pm 0.08$ | $5.56 \pm 0.19$ |
| 5 | $33.39 \pm 37.55$ | $3.57 \pm 0.28$ |

tolerance of $10^{-6}$ we note that the fixed point procedures require at most three iterations to get convergence. For example, for the ADER TT-CITA solver, third order of accuracy and NRS fixed point procedure gives $A_{NRS} + \sigma_{NRS} = 2.84$.

Table 17, shows the estimators for the non-linear system. Orders of accuracy are achieved for parameters $t_{out} = 0.1$, 128 cells, $C_{cfl} = 0.9$, $\beta = -1$ and a tolerance for fixed point iterations of $10^{-6}$. For this test, at most four iterations are carried out to get the convergence.

Notice that a tolerance $10^{-6}$ is in the range of single-precision, that roughly means seven significant decimal digits. However, this is enough to get the orders of accuracy for smooth cases. If we want to get the convergence in the range of double precision, fifteen significant digits, we have to reduce the tolerance at least to $5 \cdot 10^{-14}$. In order to have an idea about the impact of double precision and tolerance reductions into the performance of fixed point procedure, we are going to do the exercise of reducing the tolerance to $5 \cdot 10^{-14}$. Table 18 shows the results for the non-linear system, which represents the worst case and we assess the TT-RITA approach, which has more mean iterations than HEOC-RITA. Note that for fifth order of accuracy the conventional Newton method requires ten times more iterations than Newton reduced-step one.

As a summary, in all tables we note that the RITA approach has less fixed point iterations than CITA. Additionally, we note that the best performance is achieved for the linear advection–reaction case, whereas, the worst case corresponds to the non-linear system. We note that for smooth cases both fixed-point procedures achieve the orders of accuracy in at most four iterations. This suggests us that the majority of fixed point procedures could be applied in the context of implicit GRP solvers for $\epsilon = 10^{-6}$. If the tolerance is reduced to $\epsilon = 5 \cdot 10^{-14}$, the number of iterations will increase, as expected. Therefore, in order to balance the accuracy, number of fixed point iterations and thus the computational cost, in all our tests we have adopted a tolerance of $10^{-6}$.

## References


[1] D.S. Balsara, C. Meyer, M. Dumbser, H. Du, Z. Xu, Efficient implementation of ADER schemes for Euler and magnetohydrodynamical flows on structured meshes – speed comparisons with Runge–Kutta methods, J. Comput. Phys. 235 (2013) 934–969.

[2] D.S. Balsara, T. Rumpf, M. Dumbser, C.D. Munz, Efficient, high accuracy ADER-WENO schemes for hydrodynamics and divergence-free magnetohydrodynamics, J. Comput. Phys. 228 (7) (2009) 2480–2516.

[3] M. Ben-Artzi, J. Falcovitz, A second order Godunov-type scheme for compressible fluid dynamics, J. Comput. Phys. 55 (1) (1984) 1–32.

[4] R. Borsche, J. Kall, ADER schemes and high order coupling on networks of hyperbolic conservation laws, J. Comput. Phys. 273 (2014) 658–670.

[5] W. Boscheri, D.S. Balsara, M. Dumbser, Lagrangian ADER-WENO finite volume schemes on unstructured triangular meshes based on genuinely multidimensional HLL Riemann solvers, J. Comput. Phys. 267 (2014) 112–138.

[6] W. Boscheri, M. Dumbser, D.S. Balsara, High-order ADER-WENO ALE schemes on unstructured triangular meshes – application of several node solvers to hydrodynamics and magnetohydrodynamics, Int. J. Numer. Methods Fluids 76 (10) (2014) 737–778, http://dx.doi.org/10.1002/fld.3947.

[7] C.E. Castro, High-order ADER FV/DG numerical methods for hyperbolic equations, PhD thesis, Department of Civil and Environmental Engineering, University of Trento, Italy, 2007.
[8] C.E. Castro, E.F. Toro, Solvers for the high-order Riemann problem for hyperbolic balance laws, J. Comput. Phys. 227 (2008) 2481–2513.
[9] M. Dumbser, Arbitrary high order schemes for the solution of hyperbolic conservation laws in complex domains, PhD thesis, Institut für Aero- und Gasdynamik, Universität Stuttgart, Germany, 2005.
[10] M. Dumbser, Arbitrary high order PNPM schemes on unstructured meshes for the compressible Navier–Stokes equations, Comput. Fluids 39 (2010) 60–76.
[11] M. Dumbser, D. Balsara, E.F. Toro, C.D. Munz, A unified framework for the construction of one-step finite volume and discontinuous Galerkin schemes on unstructured meshes, J. Comput. Phys. 227 (2008) 8209–8253.
[12] M. Dumbser, D.S. Balsara, High-order unstructured one-step PNPM schemes for the viscous and resistive MHD equations, Comput. Model. Eng. Sci. 54 (2009) 301–333.
[13] M. Dumbser, C. Enaux, E.F. Toro, Finite volume schemes of very high order of accuracy for stiff hyperbolic balance laws, J. Comput. Phys. 227 (8) (2008) 3971–4001.
[14] M. Dumbser, A. Hidalgo, O. Zanotti, High order space–time adaptive ADER-WENO finite volume schemes for non-conservative hyperbolic systems, Comput. Methods Appl. Mech. Eng. 268 (2014) 359–387.
[15] M. Dumbser, M. Käser, Arbitrary high order non-oscillatory finite volume schemes on unstructured meshes for linear hyperbolic systems, J. Comput. Phys. 221 (2) (2007) 693–723.
[16] M. Dumbser, M. Käser, E.F. Toro, An arbitrary high order discontinuous Galerkin method for elastic waves on unstructured meshes V: local time stepping and $p$-adaptivity, Geophys. J. Int. 171 (2007) 695–717.
[17] M. Dumbser, C.D. Munz, ADER discontinuous Galerkin schemes for aeroacoustics, C. R., Méc. 333 (2005) 683–687.
[18] M. Dumbser, C.D. Munz, Building blocks for arbitrary high order discontinuous Galerkin schemes, J. Sci. Comput. 27 (2006) 215–230.
[19] M. Dumbser, O. Zanotti, A. Hidalgo, D.S. Balsara, ADER-WENO finite volume schemes with space–time adaptive mesh refinement, Commun. Comput. Phys. 248 (2013) 257–286.
[20] M. Dumbser, O. Zanotti, R. Loubere, S. Diot, A posteriori subcell limiting of the discontinuous Galerkin finite element method for hyperbolic conservation laws, J. Comput. Phys. 278 (2014) 47–75.
[21] S.K. Godunov, A finite difference method for the computation of discontinuous solutions of the equations of fluid dynamics, Mat. Sb. 47 (1959) 357–393.
[22] Claus R. Goetz, Armin Iske, Approximate solutions of generalized Riemann problems: the Toro–Titarev solver and the LeFloch–Raviart expansion, in: Proceeding of Numerical Methods for Hyperbolic Equations: Theory and Applications, Santiago Compostela, Spain, 2011, 2012, pp. 267–275.
[23] A. Harten, B. Engquist, S. Osher, S.R. Chakravarthy, Uniformly high order accuracy essentially non-oscillatory schemes III, J. Comput. Phys. 71 (1987) 231–303.
[24] M. Käser, Adaptive methods for the numerical simulation of transport processes, PhD thesis, Institute of Numerical Mathematics and Scientific Computing, University of Munich, Germany, 2003.
[25] M. Käser, ADER schemes for the solution of conservation laws on adaptive triangulations, in: Mathematical Methods and Modelling in Hydrocarbon Exploration and Production, vol. 7, Springer-Verlag, 2004.
[26] M. Käser, A. Iske, Adaptive ADER schemes for the solution of scalar non-linear hyperbolic problems, J. Comput. Phys. 205 (2005) 489–508.
[27] Ph. Le Floch, P.A. Raviart, An asymptotic expansion for the solution of the generalized Riemann problem. Part I: general theory, Ann. Inst. Henri Poincaré, Anal. Non Linéaire 5 (2) (1988) 179–207.
[28] R.J. LeVeque, H.C. Yee, A study of numerical methods for hyperbolic conservation laws with stiff source terms, J. Comput. Phys. 86 (1990) 187–210.
[29] R. Loubere, M. Dumbser, S. Diot, A new family of high order unstructured MOOD and ADER finite volume schemes for multidimensional systems of hyperbolic conservation laws, Commun. Comput. Phys. 16 (3) (2014) 718–763.
[30] G. Montecinos, C.E. Castro, M. Dumbser, E.F. Toro, Comparison of solvers for the generalized Riemann problem for hyperbolic systems with source terms, J. Comput. Phys. 231 (2012) 6472–6494.
[31] G. Montecinos, E.F. Toro, Solver for the generalized Riemann problem for balance laws with stiff source terms: the scalar case, in: Proceedings of the 13th International Conference on Hyperbolic Problems, HYP 2010, Beijing, China, June 15–19, 2010, in: Hyperbolic Problems. Theory, Numerics and Applications, vol. 2, World Scientific/Higher Education Press, Hackensack, NJ/Beijing, 2012, pp. 576–583.
[32] G.I. Montecinos, L.O. Müller, E.F. Toro, Hyperbolic reformulation of a 1D viscoelastic blood flow model and ADER finite volume schemes, J. Comput. Phys. 266 (2014) 101–123.
[33] G.I. Montecinos, E.F. Toro, Reformulations for general advection–diffusion–reaction equations and locally implicit ADER schemes, J. Comput. Phys. 275 (2014) 415–442.
[34] L.O. Müller, E.F. Toro, A global multiscale mathematical model for the human circulation with emphasis on the venous system, Int. J. Numer. Methods Biomed. Eng. 30 (7) (2014) 681–725.
[35] T. Schwartzkopff, C.D. Munz, E.F. Toro, ADER: high-order approach for linear hyperbolic systems in 2D, J. Sci. Comput. 17 (2002) 231–240.
[36] J.R. Scott, Solving ODE initial value problems with implicit Taylor series methods, Glenn Research Center, Cleveland, Ohio, 2000, NASA/TM–2000-209400.
[37] Y. Takakura, E.F. Toro, Arbitrarily accurate non-oscillatory schemes for a non-linear conservation law, Comput. Fluid Dyn. 11 (2002) 7–18.
[38] V.A. Titarev, E.F. Toro, ADER: arbitrary high order Godunov approach, J. Sci. Comput. 17 (2002) 609–618.
[39] V.A. Titarev, E.F. Toro, ADER schemes for three-dimensional hyperbolic systems, J. Comput. Phys. 204 (2005) 715–736.
[40] E.F. Toro, Riemann Solvers and Numerical Methods for Fluid Dynamics: A Practical Introduction, third edition, Springer-Verlag, ISBN 978-3-540-25202-3, 2009.
[41] E.F. Toro, R.C. Millington, L.A.M. Nejad, Towards very high-order Godunov schemes, in: E.F. Toro (Ed.), Godunov Methods: Theory and Applications, Edited Review, Kluwer Academic/Plenum Publishers, 2001, pp. 905–937.
[42] E.F. Toro, G.I. Montecinos, Advection–diffusion–reaction equations: hyperbolisation and high-order ADER discretizations, SIAM J. Sci. Comput. 36 (5) (2014) A2423–A2457.
[43] E.F. Toro, V.A. Titarev, Solution of the generalised Riemann problem for advection–reaction equations, Proc. R. Soc. Lond. A 458 (2002) 271–281.
[44] E.F. Toro, V.A. Titarev, ADER schemes for scalar non-linear hyperbolic conservation laws with source terms in three-space dimensions, J. Comput. Phys. 202 (1) (2005) 196–215.